Three-dimensional paleohistology of the scale and median fin spine of *Lophosteus superbus* (Pander 1856) (#11043)

When ready **submit your review online**. The review form is divided into 5 sections. Please consider these when composing your review:

1. **BASIC REPORTING**
2. **EXPERIMENTAL DESIGN**
3. **VALIDITY OF THE FINDINGS**
4. General comments
5. Confidential notes to the editor

🗋 You can also annotate this **pdf** and upload it as part of your review

To finish, enter your editorial recommendation (accept, revise or reject) and submit.

BASIC REPORTING

✓ Clear, unambiguous, professional English language used throughout. yes

✓ Intro & background to show context. Literature well referenced & relevant. citations missing, citations wrong, papers in references, which are not cited. And relevant citation missing.

✓ Structure conforms to **PeerJ standard**, discipline norm, or improved for clarity.

✓ Figures are relevant, high quality, well labelled & described. can be reduced (e.g. fig. 4 is a repetition of fig. 3B)

✓ Raw data supplied (See **PeerJ policy**).

VALIDITY OF THE FINDINGS

1 Impact and novelty not assessed. Negative/inconclusive results accepted. *Meaningful* replication encouraged where rationale & benefit to literature is clearly stated. not very new, repetition of Gross 1969

✓ Data is robust, statistically sound, & controlled. yes

EXPERIMENTAL DESIGN

✓ Original primary research within **Scope of the journal**.

✓ Research question well defined, relevant & meaningful. It is stated how research fills an identified knowledge gap. The authors refer to new information by 3D synchrotron data, that is only the case for the canal system, the histology is still 2D and with bad, grey pictures (less informative than Gross 1969)

✓ Rigorous investigation performed to a high technical & ethical standard. yes

✓ Methods described with sufficient detail & information to replicate. referred to Synchrotron, parameters given

✓ Conclusion well stated, linked to original research question & limited to supporting results. yes

✓ Speculation is welcome, but

should be identified as such.

The above is the editorial criteria summary. To view in full visit **[https://peerj.com/about/editorial- criteria/](https://peerj.com/about/editorial-criteria/)**

Three-dimensional paleohistology of the scale and median fin spine of *Lophosteus superbus* (Pander 1856)

Anna Jerve, Qingming Qu, Sophie Sanchez, Henning Blom, Per Erik Ahlberg

Title misleading, there is only a Two-dimensional paleohistology .. nevertheless a Three-dimensional morphology of external features and the internal canal system ….

Lophosteus superbus is one of only a handful of probable stem-group osteichthyans known from the fossil record. First collected and described in the late 19th century from the upper Silurian Saaremaa Cliff locality in Estonia, it is known from a wealth of disarticulated scales, fin spines, and bone fragments. In this study we provide the first description of the morphology and paleohistology and canal system of a fin spine and scale from *Lophosteus* using (virtual 2D thin sections and the histology is presented in bad 2D pictures) 3D reconstructions that were segmented using phase-contrast synchrotron X- ray microtomography. These data reveal that both structures have fully or partially buried odontodes (better shown in Gross 1969, figs. 12-15), which retain fine morphological details in older generations, including sharp nodes and serrated ridgelets. The vascular architecture of the fin spine tip, which is composed of several layers of longitudinally directed bone vascular canals, is much more complex compared to the bulbous horizontal canals within the scale, but they both have distinctive networks of ascending canals within each individual odontode. Other histological characteristics that can be observed from the data are cell spaces and Sharpey's fibers (I don't see how these structures can give any information about growth. The authors like Gross 1969 use the sequence of odontodes to show growth sequence) that, when combined with the vascularization, could help to provide insights into the growth of the structure. The 3D data of the scales from *Lophosteus superbus* is similar to comparable data from other fossil osteichthyans, and the morphology of the reconstructed buried odontodes (wide distributed feature, not species specific) from this species is identical to scale material of *Lophosteus ohesaarensis*, casting doubt on the validity of that species (the authors can show that on the surface strictures used to define the species). The 3D data presented in this paper is the first for fossil fin spines and so comparable data is not yet available (the authors miss the detailed growth analysis of a xenacanth spine by Soler-Gijon 1999). However, the overall morphology and histology seems to be similar to the structure of placoderm dermal plates. The 3D datasets presented here provide show that microtomography is a powerful tool for investigating the

three-dimensional canal system not microstructure of fossils, which is difficult to study using traditional histological methods (of Gross 1969 is more informative than the 2D pictures of the histology given here). These results also increase the utility of fin spines and scales suggest that these data are a potentially rich source of morphological data that could be used for studying questions relating to early vertebrate growth and evolution.

1. Three-dimensional paleohistology of the scale and median fin
2. spine of *Lophosteus superbus* (Pander 1856) [1]   [1]
3

4   Anna Jerve[1,2], Qingming Qu[1,3], Sophie Sanchez[4,5], Henning Blom[1], and Per Erik Ahlberg[1]
5

6. [1] Department of Organismal Biology, Uppsala University, Norbyvägen 18A, 752 36, Uppsala,
7. Sweden
8. [2] Biology Department, Imperial College London, Silwood Park Campus, Buckhurst Road,
9. Ascot, SL5 7PY, United Kingdom
10. [3] Centre for Advanced Research in Environmental Genomics, University of Ottawa, 20 Marie-
11. Curie, Ottawa, Ontario, K1N 6N5, Canada.
12. [4] Science for Life Laboratory and Uppsala University, Department of Organismal Biology,
13. Norbyvägen 18A, 752 36 Uppsala, Sweden
14. [5] European Synchrotron Radiation Facility, 71 Avenue des Martyrs, 38000 Grenoble, France
15

16. Corresponding author:
17

18. Anna Serve
19. Department of Organismal Biology
20. Evolutionary Biology Center, Uppsala University
21. Norbyvägen 18A
22. 752 36 Uppsala
23. Sweden
24. Email: ajerve@gmail.com
25

26. Title misleading, there is only a Two-dimensional paleohistology .. nevertheless a Three-dimensional morphology of external features and the internal canal system ….

27
28
29
30
31
32
33
34
35
36
37
38
39
40
4

50. **Abstract**
51. *Lophosteus superbus* is one of only a handful of probable stem-group osteichthyans known
52.   from the fossil record. First collected and described in the late 19th century from the upper
53.   Silurian Saaremaa Cliff locality in Estonia, it is known from a wealth of disarticulated scales,
54.   fin spines, and bone fragments. In this study we provide the first description of the
55.   morphology and paleohistology of a fin spine and scale from *Lophosteus* using 2D virtual thin
56.   sections and 3D reconstructions that were segmented using phase-contrast synchrotron X-ray
57.   microtomography. These data reveal (show what Gross 1969 has shown already) that both structures have fully or partially buried
58.   odontodes, which retain fine morphological details in older generations, including sharp
59.   nodes and serrated ridgelets. The vascular architecture of the fin spine tip, which is composed
60.   of several layers of longitudinally directed bone vascular canals, is much more complex
61.   compared to the bulbous horizontal canals within the scale, but they both have distinctive
62.   networks of ascending canals within each individual odontode. Other histological
63.   characteristics that can be observed from the data are cell spaces and Sharpey's fibers (see Gross 1969) that,
64.   when combined with the vascularization, could help to provide insights into the growth of the
65. structure (how? the authors show growth with the morphology). The 3D data of the scales from *Lophosteus superbus* is similar to comparable data
66.   from other fossil osteichthyans, and the morphology of the reconstructed buried odontodes
67. from this species is identical to scale material of *Lophosteus ohesaarensis*, casting doubt on
68.   the validity of that species. The 3D data presented in this paper is the first for fossil fin spines
69.   and so comparable data is not yet available. However, the overall morphology and histology
70.   seems to be similar to the structure of placoderm dermal plates. The 3D datasets presented
71.   here provide show that microtomography is a powerful tool for investigating the three-
72.   dimensional microstructure of fossils, which is difficult to study using traditional histological
73.   methods. These results also increase the utility of fin spines and scales suggest that these data
74.   are a potentially rich source of morphological data that could be used for studying questions
75. relating to early vertebrate growth and evolution. 76
77.
78. **Introduction**
79. Research into the early evolution of gnathostomes (jawed vertebrates) is currently undergoing
80.   a paradigm shift, with far-reaching effects including a renewed interest in the enigmatic fossil
81.   fish *Lophosteus* from the Late Silurian of Estonia. For many decades, virtually all research in
82.   the field has incorporated the assumption that the macromeric dermal bone skeleton of
83.   osteichthyans (extant bony fishes and tetrapods), that is their stable and historically conserved
84.   pattern of named bones such as maxilla and dentary, evolved directly from a micromeric
85.   ancestral condition consisting of scales or small tesserae without individual identities (Janvier
86.   1996). The similarly macromeric dermal skeleton of placoderms (jawed, armored stem-
87.   gnathostomes of the Silurian and Devonian periods) was deemed to have an independent
88.   origin from a micromeric ancestor, and any pattern matches between the placoderm and
89.   osteichthyan skeletons were interpreted as convergent. Recently, it has become clear that this
90.   hypothesis is untenable: the discovery of placoderm-like characters in the dermal skeletons of
91.   the earliest osteichthyans (Zhu et al., 1999, 2009), and in particular the Silurian "maxillate
92.   placoderm" *Entelognathus* which combines a full set of osteichthyan marginal jaw bones with
93.   an otherwise typical placoderm skeleton (Zhu et al., 2013), has demonstrated that macromery
94.   is homologous in osteichthyans and placoderms. Current consensus is that jawed vertebrates

95.   primitively have macromeric dermal skeletons, as shown by placoderms, and that this
96.   condition is retained in osteichthyans but lost in acanthodians ("spiny sharks", a Silurian to
97.   Permian group of jawed fishes) and chondrichthyans (extant cartilaginous fishes) which have
98.   become micromeric (Zhu et al., 2013; Dupret et al., 2014).

99
100
101
102
103
104
105
106
107
108
109
110
111
112
113
114
115
116
117
118
119
120
121
122
123
124
125
126
127
128
129
130
131
132
133
134
135
136

This new consensus casts a spotlight on the few macromeric fossil taxa that appear to bridge the - still quite substantial - morphological gap between placoderms and osteichthyans. These forms, which have the potential to illuminate the origin of the gnathostome crown group, include *Janusiscus* (Giles et al., 2015), *Dialipina* (not in references Schultze & Cumbaa, 2001), *Ligulalepis* (Basden et al. or and Young, 2001), *Andreolepis* (Janvier, 1968 or 1978?; Botella et al., 2007; Qu et al., 2013b) and *Lophosteus* (Pander, 1856; Gross, 1969, 1971; Botella et al., 2007), all from the Late Silurian to Early Devonian. *Janusiscus* is currently interpreted as a crownward stem gnathostome (Giles et al., 2013), the others as stem osteichthyans or unresolved basal osteichthyans (Botella et al., 2007; Zhu et al., 2013; Giles et al., 2015). While the first three genera are known from complete specimens (*Dialipina*) or braincases with attached skull roofs (*Janusiscus*, *Ligulalepis*), *Andreolepis* and *Lophosteus* are represented only by disarticulated fragments and occasional complete bones from the dermal skeleton. However, they compensate for this by the abundance of the material and in particular by the superb histological preservation of the bones (Gross, 1969, 1971; Qu et al., 2013b). This enables us to investigate the tissue organization and growth modes of their dermal skeletons, uncovering a rich source not only of paleobiological information but also of phylogenetically informative characters. The potential value of the histological data set has been greatly enhanced in recent years by the application of propagation phase contrast synchrotron microtomography (PPC- SRµCT), which allows us to visualize the histology non-destructively in three dimensions with single-cell resolution (Sanchez et al., 2012). We present here the first PPC-SRµCT investigation of the scales and dermal fin

spines of *Lophosteus*.

The scales and spines of *Lophosteus superbus* are among the most abundant remains collected from Ohessaare Cliff on the island of Saaremaa in Estonia since Pander first described this taxon in 1856. Gross (1969, 1971) provided the most detailed description of *L. superbus*, which he based on an assemblage collected from the same locality. Since then several other species of *Lophosteus* have been described from across the globe, including localities in North America (Märss et al., 1998), Australia (Burrow, 1995), and central and eastern Europe (not in references Märss, 1997; Botella et al., 2007; Cunningham et al., 2012) indicating that *Lophosteus* was widely distributed. For a more comprehensive overview of *Lophosteus* systematics, see Schultze & Märss (2004).

Because our knowledge of *Lophosteus* is based on bone fragments, scales, and spines, it has been difficult to determine precisely where it fits into the larger picture of early gnathostome evolution. However, after careful examination of the morphology and histology of the material, Gross (1969) was able to confirm that the disarticulated scales, spines and dermal bones from Ohessaare attributed to *Lophosteus* do indeed belong to one genus. *Lophosteus* is currently considered by some to be a stem-osteichthyan (Botella et al., 2007; Cunningham et al., 2012), but it has also been proposed as sharing affinities with crown osteichthyans (Gross, 1971, Rohon 1893), acanthodians (Schultze & Märss, 2004), and placoderms (Burrow, 1995). The view that *Lophosteus* is the least crownward stem- osteichthyan (Botella et al., 2007) has a significant impact on interpreting gnathostome phylogeny and the acquisition of crown gnathostome characteristics (Brazeau, 2009; Brazeau & Friedman, 2014; Giles, Friedman & Brazeau, 2015; Qu et al., 2015b).

The histology of scales and spines of early gnathostomes can reveal important information relating to the development and evolution of these structures and of the hard tissues that form them, as well as the phylogenetic relationships of the animals that carried them (not in references Ørvig, 1951, 1977; Burrow & Turner, 1999; Valiukevicius & Burrow, 2005; Schultze, 2015; Giles,

Rücklin & Donoghue, 2013). For example, *Lophosteus* and *Andreolepis* (a slightly earlier Late Silurian taxon from Gotland, Sweden) were once considered to be closely related and were grouped in the family Lophosteidae (Gross, 1969, 1971; Schultze & Märss, 2004). However, the presence of enamel in *Andreolepis* scales and the absence of this tissue

in *Lophosteus* (Gross, 1969) contributed to altering this view (Otto, 1991; Cunningham, et al., 2012; Qu et al., 2015a or b??). Given the current lack of articulated material, the scales and spines of *Lophosteus* are the most readily available source of data for phylogenetically important characters. Other bones have been identified, including jawbones (Botella et al., 2007; Cunningham et al., 2012), and a new extensive material of cranial and postcranial dermal bones from Ohessaare is currently under study (Ahlberg et al., 2013). The specimens presented here derive from this new material.

The bone histology of *Lophosteus* has been described from two-dimensional (2D) thin sections (Gross, 1969, 1971; Märss, 1986; ~~Burrow, 1995; Schultze & Märss, 2004~~ no sections) but the three-dimensional (3D) ~~histological arrangement~~ morphology and canal system of the spine and scale has never been investigated. In this paper we present detailed 3D descriptions from a fin spine and scale of *Lophosteus superbus*, based on PPC-SRµCT scans made at the European Synchrotron Radiation Facility (ESRF) in Grenoble, France. These data increase our understanding of the development of the spines and scales from this species and permit us to discuss potential new ~~paleohistological~~ characters, which will become crucial for future phylogenetic analyses.

Materials and Methods
Specimens
The material from *Lophosteus superbus* that is described in this paper was collected as part of a larger effort to amass material of Paleozoic vertebrates from Ohesaare Cliff in Estonia by Uppsala University, Sweden, and the Institute of Geology at the Tallinn University of Technology (GIT), Estonia. The material was collected from the upper Pridoli Ohesaare Cliff beds (Zigaite et al., 2015) in

large limestone blocks that were chemically prepared using a weak solution of acetic acid in water (pH 3.65) at the fossil preparation laboratory at Lund University, Sweden. Type specimens from this project are held at the GIT in Estonia and the rest of the material is housed at the Evolution Museum at Uppsala University, Sweden. 3D printed models of both specimens have been catalogued in the collection.

The ~~height~~ depth-length ratio of the scanned scale (GIT 727-1) is probably a central or anterior trunk scale based on comparison to squamation of other early osteichthyans (Chen et al., 2012; Jessen, 1968; Qu et al., 2013a or b??; Trinajstic, 1999). The scan of the scale is incomplete, missing the most dorsal and ventral part (**Fig. 1**). The *Lophosteus* fin spine (GIT 727-2) scan is also incomplete and only includes the most distal part of the structure. However, this does not affect the study of its general growth pattern and 3D architecture (see results).

Synchrotron parameters
Both the scale and the spine of *Lophosteus* (GIT 727-1 and GIT 727-2) were imaged using Propagation Phase-Contrast Synchrotron X-Ray Microtomography (PPC-SRμCT) at beamline ID19 of the European Synchrotron Radiation Facility (ESRF), France. The samples were scanned with the energy of 30 keV in monochromatic conditions, using a single crystal 2.5 nm period W/B4C multilayer monochromator. The beam was filtered with 2 mm of aluminum. The insertion device used was a U32 undulator with a gap of 12.38 mm. The detector was a FreLoN 2K14 CCD camera (Labiche et al., 2007). In association with the microscope optic and a 10 μm-thick gadolinium gallium garnet (GGG) scintillator doped with europium (Martin et al., 2009), the camera provided an isotropic voxel size of 0.678 μm. The samples were fixed at a propagation distance of 30 mm from the detector. Two thousand projections were performed during continuous rotation over 180 degrees. The time of exposure per projection was of 0.3s. The field of view at high resolution was restricted to 1.4 mm, and therefore only specific regions of the scale and spine were imaged. The data obtained in edge detection mode were reconstructed using a classical filtered back-projection algorithm (PyHST software, ESRF). Acquisition artifacts – such as ring artifacts – were

199
200
201
202
203
204
205
206
207
208
209
210
211
212
213
214
215
216
217
218
219
220
221
222
223
224
225
226
227
228
229
230
231
232
233
234
235
236
237
238
239
240
241
242
243

filtered while processing the data. Segmentation and rendering were done using the software VG StudioMax 2.2 (Volume Graphics, Heidelberg), following the protocols established by Qu et al. (2015a).

Abbreviations

al	anterior ledge
adc	ascending canal
aof	anterior overlapped field
bc	basal canal
bco	basal canal opening
bco.n	basal canal opening, not connected to the horizontal vasculature
bvc	bone vascular canals
cvc	central vascular canal
den	denteon
dt	dentine tubules
dvc	dentine vascular canals
eo	embedded odontode
fgo	first generation odontode
g (1-4)	generation(s) (1-4)
k	keel
leo	leading edge odontode
mc	median canal
o	osteocyte lacuna
pl	posterior ledge
ps	posterior surface
s	sediment
sgo	second generation odontode
shf	Sharpey's fibers
v	void spaces/pseudocanals?
vc	vascular canal
vco	vascular canal opening/pore opening

Terminology

The terminology from Gross (1969; 1971) forms the basis of our description, and most of the terms describing 2D histology are adopted ~~in 3D data~~ there is no 3D histology, only grey 2D sections. Our description of ornament and morphology follows the terminology established by Schultze and Märss (2004). General histology terms re-

garding vertebrate hard tissues follow Fran-
cillon-Vieillot et al., (1990). The homology
assessment of the canal system in 3D fol-
lows previous work on the *Psarolepis* and
Andreolepis scales (Qu et al., in press).

Description

The external morphology of the *Lophosteus*
scale (GIT 727-1) and spine tip (GIT 727-2)
described here ~~share similarities~~ are identical
with the scales and symmetrical spines that
are figured and described in Gross (1969).
The spine also shares characteristics with the
median dorsal spine described by Otto
(1991). These similarities include the overall
shape, organization of tubercles, cross-
sectional shape, morphology of the posterior
surface of the spine and the histological ar-
rangement into different tissue layers (Gross,
1969; Otto, 1991).

249
250
251
252
253
254
255
256
257
258
259
260
261
262
263
264
265
266
267
268
269
270
271
272
273
274
275
276
277
278
279
280
281
282
283
284
285
286
287
288
289
290
291
292
293

Scale Morphology and 3D Histology
Composition and overall morphology
The scale is rhombic in shape in crown view, with a broad anterior overlapped field (Fig. 1A1) no complete scale shown. There is a broad keel at the center of the scale in basal view, accompanied by an anterior ledge and posterior ledge. Numerous pores are present on the keel (Fig. 1A2). Morphologically the scanned scale conforms to the large *Lophosteus* scales as described by Gross (1969).

The histology of the scale can be subdivided into three layers, as originally recognized by Gross (1969): a basal bony layer with numerous osteocyte lacunae, a middle layer with a horizontal vasculature and osteocyte lacunae a. dentine (early odontodes) and a top layer made of dentine mainly (ornament). Besides the three main basal canals connecting with the horizontal vascular canals, there are several isolated canals in the basal layer **(Fig 1A2, 1B)**. No secondary bone deposition occurred to form osteon-like structures around these basal canals, and the bony base is made of pseudo-lamellar bone (Gross, 1969; pers. obs. by QQ based on classical thin sections). There is a peculiar loosely textured region within the basal bony layer, and this region is continuous along the length of anterior overlapped field **(Figs 1B, C)**. This loosely textured region seems to have been occupied by numerous fibers in vivo, and Sharpey's fibers extend from this region to the basal surface of the scale **(Fig 1C)**. The ornament denticles are comprised of dentine, which gradually change to cellular bone basally **(Fig 1B)**. However, there is no clear boundary between dentine and bone. The dentine of large younger odontodes becomes more complicated, with regular dentine tubules in the outer layer and denteons in the inner layer **(Fig. 2B1, 2B2)**. These denteons have a central ascending canal from which thin

tubules radiate, very similar to primary os-
teons in bony tissue, but are composed of
dentine **(Fig. 2B2)**.that depends where you
cute odontode, I see bone cells in the dent
eons in Fig. 2B2see also the canals in Gross
1969, gigs. 12B, 13A, 14A, B.

Ornamentation
Although the scan is incomplete, missing a
small dorsal portion and a ventral portion of
the scale **(Fig 1)**, it is possible to reconstruct
the growth history of the scale crown by
rendering the embedded odontodes **(Fig 3)**.
Four generations of odontodes have been
identified. Each generation consists of mul-
tiple odontodes, which share the same bony
base **(Fig 3A)** and are similar in size and
shape **(Fig 3B)**. Odontodes of each genera-
tion form a continuous sheet and are con-
nected by bony tissues. Odontodes of a
younger generation never cover the previous
generation odontodes completely, conform-
ing to an areal growth pattern.

First generation odontodes are triangular in
crown view, with two major (middle)
ridgelets converging to the posterior tip on
each odontode **(Fig 3B1)**. There is a long
ridgelet with nodular serrations on the ven-
tral side of each odontode **(Fig 4A1)**, but the
number of nodules varies. Second genera-
tion odontodes are larger and more elongat-
ed than first generation odontodes. There al-
so are more ridgelets on each odontode, with
dorsal and ventral ridgelets having nodular
serrations **(Figs 3B2, 4A2)**. Nodules become
more prominent basally on each ridgelet. In
posterior view each odontode is stellate-
shaped with ridgelets radiating from the pos-
terior tip **(Fig 4A2)**. Third and fourth gener-
ation odontodes are larger than older odon-
todes. Their posterior tips become blunt,
suggesting strong postmortem erosion.
There are more ridgelets on these odontodes
than on older odontodes. Nodular serrations
on embedded part of ridgelets are clearly
visible, while remnants of nodules after ero-
sion become faint on exposed surfaces **(Fig
4A3)**.fig. 3A-B1-5 show the same as fig.

4A1-4, one can bee omitted

Vascularization
The whole canal system is subdivided into three
parts: 1. A basal part with vertical basal
canals in the bony base **(Fig 5, yellow)**; 2. A
middle part with horizontal canals lying be-
low odontodes **(Fig 5, pink and green)**; 3. A
crown part with vertical ascending canals
(surrounded by "denteons") lying within
odontodes **(Fig 5B, bright red)**. This divi-
sion is consistent with the three layers of 2D

299
300
301 histology of the scale. The middle horizontal canals have numerous openings **(Fig 5, green)** on the surface of the scale. (Gross 1969, fig. 11)

There are three basal canals connecting with the middle horizontal canals **(Fig 5)**, but several isolated basal canals that do not connect with other canals are also present (bco.n in **Fig 1A2**). The middle horizontal canal system consists of bulging sack-like cavities joined together by much narrower canals that show semi-regular spacing **(Fig 5A)**. Except where overgrown by later odontodes, these narrow canals (green) open onto the external surface of the scale through a ring of foramina around the base of each odontode (Fig. 1E). Since the ascending canals (Fig. 5, bright red) originate from the middle canals and connect to terminal dentine tubules within odontodes, the middle horizontal canals are considered as vascular canals too. Each odontode overlies a sack-like cavity of the middle horizontal canal system, and younger larger odontodes have correspondingly larger horizontal cavities below them **(Fig 5A2-A5)**. Within the odontodes some ascending canals connect with each other by forming arcade-like structures ("*Arkadenkanal*" in Gross, 1969) **(adc, Fig. 5)**. Dentine tubules originate from the ascending canals and arcade canals that should thus be considered as pulp canals proper or cavities.

Spine Tip Morphology and 3D Histology
Composition and overall morphology
The spine is constructed of dermal bone that is covered ~~in~~ by dentine odontodes **(Fig 6A1-4)**. The lateral sides of the spine are ornamented in asymmetrical stellate tubercles, or odontodes, that are ornamented with "ridgelets", as described in Märss et al. (1998) and Schultze and Märss (2004) **(Fig 6B)**. Odontodes can be partially overlapping or freestanding with the former being small-

er and shorter than those that are freestanding **(Fig 6A2; compare Fig 8E to Fig 8F)**. There are many pores that represent vascular canal openings located on the surface of the spine, usually between odontodes on the lateral sides of the spine **(Fig 6B, 6C; vco)**, and parallel with the edges of the posterior surface (ps) of the spine **(Fig 6A3)**. They are typically not as regularly arranged, or as closely associated with individual odontodes, as the corresponding pores on the scales. Similar to the observations of Otto (1991) and Gross (1969), we note that the leading edge of the spine is constructed of a linear row of slightly offset, elongated and unornamented odontodes **(Fig 6A1-2, 4, 6C; leo)**. The posterior surface of the spine is constructed of bone, bears no odontodes, and is narrower than the lateral sides **(Fig 6A1-4)**. The bony part of the spine along its posterior surface is slightly concave with short ridges running along the sides **(Fig 6A3)**. The ridges fade and flatten out distally and the surface narrows to a rounded boundary, which demarcates the bone from a dentine tubercle that comprises a portion of the tip of the spine **(Fig 6A3-A4)**, along with the odontode at the spine tip's leading edge (between the lateral faces of the spine) **(Fig 6A4)**.

Ornamentation
Overlapping odontodes like those noted by Gross (1969) and Otto (1991) can be seen on the scan data and have been reconstructed here **(Figs 7-8)**. Individual odontodes are elongate with a ridge that extends the length of each structure. Ridglets extend toward the base of the odontodes and from the median surface of the structure to form an overall stellate pattern. These odontodes are classified as either first- or second-generation as their relative ages can be determined **(Figs 7-8)**. Second generation odontodes (sgo) are younger and they share the outer bone surface as a depositional boundary **(Figs 7A1-2, 7B, 7C1, 7C3)**. These tubercles tend to be larger and longer with broad, smooth surfac-

es and ridgelets, relative to the older first generation tubercles **(Fig 8F1-3, 8G1-3)** (fgo) that are partially buried **(Fig 7A1-2, 7B, 7C1-2)**. These first generation tubercles share a depositional surface under the bony surface of the spine **(Fig 7A1-2, 7C2)**. The buried first generation tubercles are ornamented with a series

349
350
351   of diagonally crossing sharp ridgelets of dif-
352   ferent lengths **(Fig 8D1-4; 8E1-4)**. A series
353   of tooth-shaped nodules that form rough ser-
354   rations can be seen on the distal end of these
355   tubercles **(Fig 8E1-4; yellow arrow)**.
356
357   *Overall histology*
358   Gross (1969) and Otto (1991) described the
359   2D histology of the spine similarly to that
360   of the scale, including a lamellar bony layer
361   that bears longitudinal canals, a middle
362   "spongy" layer, and an ornamented dentine
363   layer. Here, we identify a more compact
364   bone with fewer bone cell spaces **(Fig 6C;
365   blue)**, a layer of bone with many bone cell
366   spaces, pseudocanals, and void spaces **(Fig
367   6C; purple)**, and an outer ornamented den-
368   tine layer **(Fig 6; red)**. Additionally, the
369   bony posterior region of the spine contains
370   numerous Sharpey's fibers for attachment
371   with the fin **(Fig 6C; green)**. The dentine
372   layer is not continuous over the surface of
373   the spine.all much better visible in Gross
374   1969, fig. 14A.
375
376   *Vascularization*
377   Vascular canals (vc) within the body of the
378   spine surround a large central vascular ca-
379   nal (cvc), which is non-uniform and roughly
380   triangular in cross-section and appears to be
381   composed of several "lobes" **(Fig 9)**. Canals
382   which we designate as bone vascular canals
383   **(Fig 9A; bvc1, teal/blue)** bifurcate from the
384   central vascular canal **(Fig 9A; cvc, or-
385   ange)** and are associated with the main
386   bony core of the spine. Near the central
387   vascular canal, this layer consists of long
388   and narrow canals that are closely situated
389   together. Distally, these canals become
390   smaller in size and are more rounded in
391   cross-section **(Fig 9A)**. Bone vascular ca-
392   nals meet posteriorly at a large median ca-
393   nal **(Fig 9A; mc, purple)** that runs longitu-
394   dinally along the length of the central vas-
       cular canal. The median canal is the second

largest component of the vascular network, with many laterally bifurcating arms. Large bone vascular canals connect the median canal to the central vascular canal anteriorly in places but these can also be connected directly to each other **(Fig 9A, B)**. Smaller canals connect the median canal posteriorly to the basal canal **(Fig 9A; bc, yellow)**. The basal canal is narrower than the median canal and also runs the length of the central vascular canal **(Fig 9B-D)**. At the distal end of the spine tip this canal bifurcates into several smaller canals that form some of the vascular network of the tip of the spine **(Fig 9C, 9D; pink; yellow arrows)**. The second layer of bone vascular canals **(Fig 9; dvc2, pink)**, are outermost in position and are associated with the outermost layer of bone that has many cell and void spaces **(Fig 9B)**. They typically have a clear boundary with the rest of the vascular network, which is marked by short, thin canals **(Fig 9A, B)**. The vascular network of the most distal part of the tip of the spine is continuous with the vascular network of the spine body, but all of the layers converge leaving no clear boundaries **(Fig 9C-D)**.

Some odontodes contain their own smaller vascular network, composed of what are designated here as ascending canals **(Fig 10; adc)**. Ascending canals form a well-developed, complex network of looping vascular canals involved with the deposition of each odontode. The canals of the network attach to the outer layer of bone vascular canals basally to create a loop distally, whose height reflects the overall morphology of each individual odontode (**Fig 10E2,3**). Branching dentine tubules can be reconstructed and can be observed on the most distal parts of the loops **(Fig 10D1,E1; marked by yellow arrows)**. The details of the ascending canals are best observed in second generation odontodes (younger odontodes), because unlike those of first generation odontodes (older odontodes) they have not been secondarily filled by dentine (**compare 10D**

to 10E). What do you mean with secondary dentine? secondary dentine looks different. Here it is a question of the direction of the section.

399
400
401 *Cell distribution*
402 Bone cell spaces are dispersed around the
403 vascular canals and throughout the bony part
404 of the spine **(Fig 11A, B)**. There appears to
405 be a lower density of cell spaces immediate-
406 ly proximal to the central vascular canal in
407 virtual thin sections of the data **(Fig 11A)**.
408 Clusters of what appear in cross-section to
409 be bone cell spaces are also present and are
410 all located around the outer 2/3 of the bone
411 layer, but these are difficult to identify as
412 such when rendered in 3D **(Fig 11A, C-G)**.
413 Some of the more enigmatic spaces resem-
414 ble vascular canals with pocked surfaces
415 **(Figs 11C-E, G)**, while others render as un-
416 identifiable voids **(Fig 11F)**. The latter are
417 most likely fiber bundles.
418 Irregularly shaped canals, referred to
419 as void spaces/pseudo-canals (v) here, are
420 also located in ring around the outer 2/3 of
421 the bone layer **(Fig 12)**. In section images
422 the pseudo- canals look like vascular canals
423 **(Fig 12A-C)**, but when they are rendered in
424 3D they appear to be irregularly shaped,
425 mostly flat, and do not seem to connect to
426 any of the vascular canals **(Fig 12D-F)**. In
427 some respects, they resemble the large clus-
428 ters of unidentifiable cell spaces mentioned
429 above **(Fig 11C, G)**. The pseudo-canals ap-
430 pear to be located in one layer in the bone
431 and are seen regularly throughout the scan of
432 the spine **(Fig 12D, E)**.
433
434 *Attachment fibers*
435 Sharpey's fibers are present in the scan data of the
436 posterior surface of the spine **(Fig 6; shf,**
437 **green & Fig 13)**. In cross-section these are
438 more closely spaced together than the cell
439 spaces in Figure 11, and they are limited to
440 the area around the posterior surface of the
441 fin spine **(Fig 13A-D)**. The fibers are elon-
442 gated and intersect and exit the surface of
443 the spine at an angle **(Fig 13C-G)**. They are
444 difficult to segment and are often not clear-
ly separable from cell spaces.

PeerJ

Discussion

Assigning the material to Lophosteus superbus
Lophosteus superbus was originally diagnosed by Gross (1969) from scales, fin spines, and other bony fragments, all which bear round or elongated stellate odontodes. The scale and spine material described here matches the description provided by Gross (1969) and Schultze
& Märss (2004). The morphology of the scale is rhombic and it is ornamented with a series of obliquely placed set of overlapping ridges that do not form a continuous layer of dentine layer (Gross, 1969; Schultze & Märss, 2004). The results of the 3D data presented here have some implications on the taxonomic status of the species *Lophosteus ohesaarensi*s, described from the Ohesaare Cliff locality by Schultze & Märss (2004). *L. ohesaarensis* was distinguished from *L. superbus* by the morphology of the ridglets that comprise the individual odontodes on the scales. Schultze and Märss (2004) provided three diagnostic characters for *L. ohesaarensis*, including, 1., scales with fine parallel ridgelets on crest, which is the highest line of the ridge, ridgelets change angle from 10° to nearly 90° to crest on lateral sides of the ridges; 2., lower part of ridgelets with nodular serrations; 3., anterior overlapped field weakly pustulate. The first two characters are clearly visible in the second-generation odontodes of the described scale **(Figs. 3B2, 4A2)**. Regarding the third character, the anterior overlapped field is less pustulate in the young scale with the first generation odontodes **(Fig. 3B1)** compared to the mature scale **(Fig. 3B5)**. The scales described as *L. ohesaarensis* are generally smaller with less prominent anterior overlapped field, which suggests that they are most probably juvenile scales of *L. superbus*. Gross (1969) also has described several scales with small anterior overlapped fields. It is thus more likely that

there is only one valid species of *Lophosteus* from the Ohesaare Cliff locality. However, a similar examination of different

448
449
450
451
452
453
454
455
456
457
458
459
460
461
462
463
464
465
466
467
468
469
470
471
472
473
474
475
476
477
478
479
480
481
482
483
484
485
486
487
488
489
490
491
492

ontogenetic stages of *L. superbus* and *L. ohesaarensis* material collected from the Ventspils borehole, Latvia, is necessary to confirm their taxonomic status.

Up to eight types of spines and spine-like elements have been attributed to *Lophosteus*, including symmetrical and asymmetrical forms that are associated with median and paired fins, respectively. The original diagnosis of *L. superbus* made by Gross (1969) includes a symmetrical spine that is triangular in cross-section with parallel ridges of stellate odontodes that meet at the leading edge. Symmetrical spines recovered from Saaremaa have a similar odontode arrangement, in addition to having rows of ridge-like tubercles that are in parallel row on the lateral parts of the spine and have a long base (Schultze and Märss, 2004). These descriptions differ from the median dorsal spine presented by Otto (1991), who reported that odontodes on the lateral sides of the spine were of varying sizes and not arranged in distinct parallel rows. Otto (1991) noted that leading edge is composed of ridge- like odontodes that are arranged into a single linear row, which was also figured by Gross (1969). It is challenging to assign the spine tip described here to one type of spine because the scan data only represents the most apical region of the structure, but some comparisons can be made (Fig 6). The spine tip shares a large number of similarities with the symmetrical spines and median dorsal spine of *L. superbus* material already described by Gross (1969), Otto (1991), and Schultze and Märss (2004). The posterior surface of the spine tip is unornamented and slightly concave base-ward and slightly convex to flat at the tip, which is similar to the same surfaces in *L. superbus* spines described by Gross (1969) and Schultze & Märss (2004). Moreover, the scan data show the multiple generations of odontode growth that are included in the

original descriptions by Gross (1969) and the later description by Otto (1991). Overall, the spine tip described in this paper is most similar to the median dorsal spines described by Otto (1991) and Gross (1969) on the basis on the arrangement of the ridge-like odontodes comprising the leading edge. However, there ~~is~~ are no data (plural!) for the proximal part of this spine and so it is difficult to say this with complete certainty.

Lophosteus Spine and Scale Histology Comparison
The 3D reconstructions of the current data have revealed several new characters that are shared between the scale and the spine of *Lophosteus* that otherwise might not have been identified through traditional investigation. Datasets confirm the earlier descriptions made by Gross (1969) with the spine and scale being constructed similarly, with a loosely calcified bony base that is covered in dentine odontodes **(Figs 1 & 6)**. Within the bony tissue we have identified large void spaces that most likely represent clusters of fibers **(Fig 1B-D & 11)**. We also validate the claim that the surface of each structure is not covered by a continuous layer of dentine (Gross 1969); rather, bony surfaces can be identified between each odontode **(Figs 1E & 6B).** The exposed bony surfaces of the scale and spine seem to bear osteoblast spaces, while osteocyte lacunae can be identified from virtual thin sections. The osteocyte spaces are uniquely large in size and may help as a diagnostic tool in future studies **(Figs 7A1 & 11)**. Another feature that we can confirm from these data is the presence of a large amount of Sharpey's fibers connected to the ventral surfaces of both the spine and the scale **(Figs 1, 6C, 13)**.

Our data further agree with Gross (1969) and Otto (1991) with regard to the presence of overlapping odontodes. The overall morphology of each odontode - elongate, stellate, and ridged - is the same on both scale and spine **(Figs 3 & 8)**. We have shown that

the scale has four generations of odontode deposition allowing for both partially and fully buried odontodes, while the spine tip bears only two generations of odontodes, with one partially buried generation, that are confined to the most posterior part of the lateral surfaces. Currently it is impossible to say whether the spine possesses more generations of odontodes basally, but this idea cannot be ruled out completely without further investigation.

498
499
500
501
502
503
504
505
506
507
508
509
510
511
512
513
514
515
516
517
518
519
520
521
522
523
524
525
526
527
528
529
530
531
532
533
534
535
536
537
538
539
540
541
542

Ridgelets that provide ornamentation on individual odontodes are similar between the scale and the spine. The features on youngest generation odontodes are rounded with the median ridgelet on each being wide and smooth, ending in a point (Figs 3, 4, & 8). Older generations of odontodes share that same morphology, but have sharper features. The smoother ridgelets of the youngest generation odontodes are most likely due to erosion as both rounded and sharp ridges can be observed on the same odontode depending on whether the surface is buried. Ridgelets extend from the median ridgelet and surround the entire circumference of each odontode on the scales. The spine odontodes have a similar overall organization, but the ridgelets on buried surfaces have a more random distribution and do not become nodular proximally. The other spine odontodes do not preserve these nodules, probably because they are not fully buried and have been eroded.

The vascularization of the spine and scale of *Lophosteus* share some similarities, but are generally quite different. Overall, the spine has a more complex vascular system than the scale. The spine tip has a multi-tiered vascular system for the bony base and several individual systems for each odontode. The scale also has bulbous and rounded vascular systems for each odontode (**Fig 5B**), but there is no central system within the bone itself. Instead, the scale has several basal canals that exit the base. The spine tip also has a basal canal but it is difficult to comment any more on that without more proximal scan data. Both the spine and the scale have ascending vascular canals within each odontode. The ascending canals in the scale are attached to the bulbous pulp cavity of each odontode (**Fig 5B**). This is also true for the spine, but these odontodes are not fed by bulbous pulp cavities (**Fig 10**); instead,

they are attached to the outermost bone vascular canals. However, the ascending canals in the spine are only open in the youngest odontodes, which are only located near the posterior margins of the spine and not evenly distributed over the entire surface (Fig 10). A full scan of the *Lophosteus* spine is required to understand the odontode distribution and vascularization.

Both the spine and the scale have many vascular pore openings at the bone surface, as first suggested by Märss (1986) **(Fig 6)**. These can also be observed on the dentine depositional surfaces of buried odontodes. There is a second-generation odontode on the spine tip that has a pore opening on its surface connected to the ascending canals within it **(Fig 8F1)**. This feature is unique to that particular odontode and cannot be observed elsewhere on the spine and is most likely the result of weathering.

Comparison of the scale and spine of Lophosteus to other taxa
Rohon (1893) described scales of *Lophosteus* for the first time and considered this taxon as a sarcopterygian. Gross (1969) identified *Lophosteus* as an early osteichthyan that cannot be assigned to either actinopterygians or sarcopterygians, based on the shape and histology of scales and spines. It is the third osteichthyan for which detailed 3D histological data have been obtained from the scales, the other two being *Andreolepis* (Qu et al., 2013b) and *Psarolepis* (Qu et al., in press).

The morphology of *Lophosteus* scales is consistent with known osteichthyan scales, with a rhomboid shape, peg-and-socket structure and an anterior overlapped field (Schultze, 2015). The lack of enamel on the scale surface of *Lophosteus* does not result from post-mortem erosion, as the embedded odontodes (which have not been subjected to post-mortem erosion) confirm the absence of an enamel layer on top of the dentine. *Lo-*

phosteus is the only known osteichthyan that has a dermal odontode skeleton entirely devoid of enamel, a characteristic that supports its placement in the osteichthyan stem group (Qu et al., 2015b).

The scale crown is composed of four generations of odontodes. All figured scales of *Lophosteus* show each generation consisting of more than one odontode. The odontodes from a given generation are not in contact with each other, and their contact with the underlying

548
549
550
551
552
553
554
555
556
557
558
559
560
561
562
563
564
565
566
567
568
569
570
571
572
573
574
575
576
577
578
579
580
581
582
583
584
585
586
587
588
589
590
591
592

odontodes of the previous generation is mediated by bone of attachment; there is no direct dentine-on-dentine contact. This is different from the pattern of *Psarolepis* scales and *Andreolepis* scales, in which the odontodes are in direct contact with each other by dentine, sometimes united by a shared enamel layer, and are added one at a time so that they cannot really be grouped into generations unless you consider each "generation" to contain just one odontode (Qu et al., 2013b; Qu et al., in press). The morphology of first generation odontodes in *Lophosteus* is similar to the first (primordial) odontode of *Andreolepis* scales (Qu et al., 2013b), with a pointed posterior end and a slender triangular shape. However, *Lophosteus* odontodes have more ridgelets posteriorly and these ridgelets bear several nodules forming serrations **(Fig. 4A1)**, similar to younger odontodes. Although the most superficial odontodes are heavily eroded and such serrations become faint **(Fig. 4A4)**, all embedded odontodes show such serrations clearly **(Fig. 4A1-A3)**. The ridgelets on odontodes (either embedded or exposed) of *Andreolepis* and *Psarolepis* are smooth and have no such serrations with protruding nodules. On the other hand, such serration is common in some placoderm scales, such as *Romundina* (not in references Ørvig, 1975). The nodules on serrations are delicate structures and can be easily destroyed by postmortem erosion, making it difficult to evaluate the feature in other placoderms. Thus more placoderm scales (especially from articulated specimens) need to be scanned to reconstruct embedded odontodes.

The organization of the canal system in *Lophosteus* is similar to that of the *Andreolepis* scale. In the bony base there are three canals connected with a horizontal vascular network. All three basal canals are tilted anteriorly, similar to *Andreolepis* and *Psarolepis* scales. In addition, there are

several isolated canals that do not connect with any other canals. No such isolated canals are found in *Andreolepis* or *Psarolepis* scales (Qu et al., in press). The horizontal vascular canals are much thicker than those of *Andreolepis* and *Psarolepis* scales, especially for the bulbous canals under large young odontodes (**Fig. 5A4-A5**). The horizontal vascular canals are flattened (**Fig. 5A6**) in basal view in all three taxa.

While there is a small amount of directly comparable synchrotron data (Qu et al., 2013b; Qu et al., in press) for the *Lophosteus* scale, there is none yet published relating to the spine. There are, however, a large number of 2D histological descriptions of early vertebrate spines (not in references Jerve et al. 2014; not in references Burrow et al. 2016) that can be compared to the thousands of virtual thin sections that comprise a synchrotron dataset, some of which we will briefly summarize here. However, it is not possible to comment in great detail on the morphology of structures that are only known from the 3D reconstructions (i.e., details relating to buried surfaces and individual odontode morphology, 3D architecture of the vascular canals).

The composition of the acanthodian and chondrichthyan fin spines is different from *Lophosteus.* Acanthodian fin spines (*Climatius*, *Parexus*) are composed of osteodentine and mesodentine, with some lacking cellular bone (Burrow et al., 2010; Burrow et al., 2013; Burrow et al., 2015) while others have it (*Nostolepis*; not in references Denison, 1979). Fin spines of fossil and extant chondrichthyans differ even more from *Lophosteus* in that they lack bone altogether and are composed of different proportions of lamellar osteodentine and trabecular dentine that can be covered to varying degrees in mantle dentine and enameloid, depending on the taxon (not in references Maisey, 1979; not in references Jerve et al., 2014). In extant (and probably in fossil) chondrichthyans, the tips of the spines are shaped by an intitial epithelial fold, which defines the outer surface of

the mantle dentine. This dentine grows centripetally, deposited by odontoblasts that differentiate from the mesenchyme contained within the epithelial fold; in effect the tipregion of the spine behaves like a single large odontode. The trunk dentine, which can comprise both lamellar and trabecular parts, develops within the mesenchyme of the spine primordium without contact with an epithelium (M not in references Maisey, 1975; not in references Jerve et al., 2014). The histology of the *Lophosteus* fin spine tip shows compositional similarity with the dermal plates of acanthothoracid placoderm fish (Giles et al. 2013), but the vascularization in the tip of the spine suggests that

598
599
600
601
602
603
604
605
606
607
608
609
610
611
612
613
614
615
616
617
618
619
620
621
622
623
624
625
626
627
628
629
630
631
632
633
634
635
636
637
638
639
640
641

the oldest part of the spine includes the tip. However, scan data taken from the midline and base of the spine are necessary to confirm this.

The odontode sculpture of *Lophosteus* is similar to the ornamentation found on acanthothoracid placoderms, like *Romundina stellina* (not in referencesØrvig 1975). The ornamentation on most acanthodian spines appears to be more linear and continuous along the length of the spine (Miles, 1973), but there are some taxa that bear linear ridges that transform into nodules toward the base (Burrow et al., 2015). In the acanthodian *Gyracanthides murrayi* the pectoral fin spines have ornamentation where the individual nodules bear a stellate arrangement of ridges and somewhat resemble the ornament odontodes of *Lophosteus* and acanthothoracids (Warren et al., 2000). This ornament morphology was also reported by Miles (1973) to be present on the pectoral spines of the acanthodian *Vernicomacanthus uncinatus*. However, unlike in *Lophosteus* this ornament always seems to consist of a single layer, with no suggestion of multiple generations of odontode formation.

Some chondrichthyan fin spines share the acanthodian type of ornamentation with certain fossil sharks such as *Asteracanthus* and other hybodonts having a very thick layer of dentine ornament, but this has been greatly reduced in extant species like *Heterodontus*, *Squalus*, and *Callorhinchus milii* (not in references Jerve et al., 2014). Tooth-like nodules are also present on acanthodian and chondrichthyan dorsal fin spines and are usually located on the most apical part of the posterior side, or trailing edge. In *Gyracanthides murrayi* and *Callorhinchus milii*, they are positioned in rows and are independent of any linear ridging and/or nodular ornamentation on the lateral sides of the spines (Warren et al., 2000; not

Jerve et al., 2014). This feature is not present on any of the *Lophosteus* spines. *Lophosteus* also differs from chondrichthyans and acanthodians in its distinct posterior spine surface and the extent of the attachment fibers (Sharpey's fibers) in this area. This surface, which must have formed the attachment for the fin, extends all of the way to the spine apex, indicating that the spine did not have a projecting free tip like in *Callorhinchus*, *Squalus*, or acanthodians. Rather, the spine may have formed with the purpose of providing support for the leading edge of the fin.

Conclusions

The description of the scale and spine tip of *Lophosteus* presented here shows that there is a ~~great~~ deal of histological information that can be derived from ~~high-resolution~~ 2D datasets. Not only are we able to confirm the previously published characteristics from this taxon by Gross (1969) and others, but we have also shown that 3D synchrotron data can aid in identifying new morphological and arrangement of vessels ~~potentially important paleohistological~~ features. The large number of histological similarities between the scale and the spine imply that these are characteristics that could be used for phylogenetic analysis as well as studying biological processes and development. Because of the current limited availability of comparable 3D data (Qu et al., 2013b; Qu et al, in press), we have elected not to attempt a phylogenetic investigation or definition of discrete characters at this stage, but we are confident that the continuing rapid expansion of this data set with the description of new early vertebrate histologies will eventually have a profound impact on our understanding of deep vertebrate interrelationships.

Acknowledgments

648
649
650
651
652
653
654
655
656
657
658
659
660
661
662
663
664
665
666
667
668
669
670
671
672
673

References

Ahlberg PE, Blom H, Zhu M, Märss T, Sanchez S. 2013. Osteology and morphology of the probable stem-group osteichthyan *Lophosteus superbus* Pander, from the Silurian of Estonia. Society of Vertebrate Paleontology 76th annual meeting abstract volume. p. 73.

not cited or Basden et al.? Basden AM, Young GC. 2001. A primitive actinopterygian neurocranium from the Early Devonian of southeastern Australia. *Journal of Vertebrate Paleontology* 21: 754–766.

Botella H, Blom H, Dorka M, Ahlberg PE, Janvier P. 2007. Jaws and teeth of the earliest bony fishes. *Nature* 448:583–586 DOI:10.1038/nature05989.

Brazeau MD. 2009. The braincase and jaws of a Devonian 'acanthodian' and modern gnathostome origins. *Nature* 457:305–308 DOI:10.1038/nature07436.

Brazeau MD, Friedman, M. 2014. The characters of Palaeozoic jawed vertebrates. 2014. *Zoological Journal of the Linnean Society* 170(4):779-821 DOI: 10.1111/zoj.12111.

Burrow CJ. 1995 A new lophosteiform (Osteichthyes) from the Lower Devonian of Australia. *Geobios Memoire Special* 19:327–333.

Burrow CJ, Turner S. 1999. A review of placoderm scales ad their significance in placoderm phylogeny, *Journal of Vertebrate Paleontology* 19(2):204-219.

Burrow CJ, Desbiens S, Ekrt B, Südkamp WH. 2010. A new look at *Machaeracanthus*. In: *Morphology, Phylogeny and Paleobiogeography of Fossil Fishes*, DK Elliott, JG Maisey, X Yu, D Miao (eds.):59-84. town, publisher

not cited Burrow CJ, Turner S. 2010. Reassessment of "*Protodus*" *scoticus* from the Early De-vonian of Scotland. *Morphology, Phylogeny and Paleobiogeography of Fossil Fishes*, DK Elliott, JG Maisey, X Yu & D Miao (eds.):123-144.

Burrow CJ, Newman MJ, Davidson RG, den Blaauwen.first name? 2013. Redescription of *Parexus recurvus*, an Early Devonian acanthodian from the Midland Valley of Scotland. *Alcheringa: an Australasian Journal of Palaeontology* 37(3): 392-414.

Burrow CJ, Davidson RG, den Blaauwen JL, Newman MJ. 2015. Revision of Climatius reticulatus Agassiz, 1844 (Acanthodii, Climatiidae), from the Lower Devonian of Scotland, based on new histological and morphological data. *Journal of Vertebrate Paleontology* 35(3):DOI: 10.1080/02724634.2014.913421.

Chen D-L, Janvier P, Ahlberg PE, Blom H. 2012. Scale morphology and squamation of the Late Silurian osteichthyan *Andreolepis* from Gotland, Sweden. *Historical Biology* 24(4):411- 423.

703
704 Cunningham JA, Rücklin M, Blom, H, Bo-
705 tella, H, Donoghue, PCJ. 2012. Testing
706 models of dental development in the earli-
707 est bony vertebrates, *Andreolepis* and *Lo-*
708 *phosteus*. *Biology Letters*,
709 DOI:10.1098/rsbl.2012.0357.
710
711 not cited Dupret V, Sanchez S, Goujet D,
712 Tafforeau P, Ahlberg PE. 2010. Bone vas-
713 cularization and growth in placoderms
714 (Vertebrata): The example of the premedian
715 plate of *Romundina stellina* Ørvig, 1975.
716 *Comptes-rendus Palevol* 9: 369-375.
717
718 Dupret V, Sanchez S, Goujet D, Tafforeau
719 P, Ahlberg PE. 2014. A primitive placo-
720 derm sheds light on the origin of the jawed
721 vertebrate face. *Nature* 507(7493):500-503.
722
723 Francillon-Vieillot H, de Buffrénil V, Casta-
724 net J, Gérauldie J, Meunier FJ, Sire J-Y,
725 Zylberberg L, de Ricqlès A. 1990. Micro-
726 structure and mineralization of vertebrate
727 skeletal tissues. In: Carter JG, editor. *Skele-*
728 *tal biomineralization: patterns, processes*
729 *and evolutionary trends*. New York: Van
730 Nostrand Reinhold. p 471-530.
731
732 not cited Friedman M, Brazeau MD. 2010.
733 A reappraisal of the origin and basal radia-
734 tion of the Osteichthyes. *Journal of Verte-*
735 *brate Paleontology* 30(1):36–56.
736
737 not cited Friedman M, Brazeau MD. 2013. A
738
739 jaw-dropping fossil fish. ~~*Palaeontology Na-*~~
740
741 ~~*ture*~~ 502:175-177.
742

Giles S, Rücklin M, Donoghue PCJ. 2013.

Histology of ''Placoderm'' Dermal Skele-

tons:
Implications for the Nature of the Ancestral Gna-

thostome. *Journal of Morphology* 274:627-644.

not cited Gross W. 1968. Fragliche Actinopterygier-Schuppen aus dem Silur Gotlands. *Lethaia* 1:184- 218.

Giles S, Friedman M, Brazeau M. 2015. Osteichthyan-like cranial conditions in an Early Devonian stem gnathostome. *Nature* 520:82-85 DOI:10.1038/nature14065.

Gross W. 1969. *Lophosteus superbus* Pander, ein 'Teleostome aus dem Silur Oesels. *Lethaia* 3:15-47.

Gross W. 1971. *Lophosteus superbus* Pander: Zaehne, Zahnknochen und besondere Schuppenformen, *Lethaia* 4:131-152.

not cited Janvier P. 1978. On the oldest known teleostome fish *Andreolepis hedei* Gross (Ludlow of Gotland), and the systematic position of the lophosteids. *Eesti NSV Teaduste Akadeemia Toimetised, Geoloogia* 27(3):88–95.

Janvier, P. 1996. *Early vertebrates*. Clarendon Press, Oxford, 393 pp.

Jessen HL. 1968. *Moythomasia nitida* Gross und *M*. cf. *striata* Gross, Devonische Palaeonisciden aus dem oberen Plattenkalk der Bergisch-Gladbach - Paffrather Mulde (Rheinisches Schiefergebirge). *Palaeontographica Abt A* 128:87-114.
Labiche JC, Mathon O, Pascarelli S, Newton MA, Ferre GG, Curfs C, Vaughan F, Homs A, Carreiras DF. 2007. The fast readout low noise camera as a versatile X-ray detector for time resolved dispersive extended X-ray absorption fine structure and diffraction studies of

746
747
748 dynamic problems in materials science,
749 chemistry, and catalysis. *Review of Scien-*
750 *tific Instruments* 78(9):091301-091311.
751
752 Miles, R. S. 1973. Relationships of acanthodians.
753 63–103. *In* Greenwood, P. H., Miles, R.
754 S. and Patterson, C. (eds). *Interrelationships of*
755 *fishes*. Academic Press, London, 536 pp.
756
757 not cited Miller RF, Cloutier R, Turner S.
758 2003. The oldest articulated chondrichthyan
759 from the Early Devonian period. *Nature*,
760 425, pp. 501–504
761 DOI:10.1038/nature02001.
762
763 Martin T, Douissard P-A, Couchard M, Cecilia A,
764 Bumbach T, Dupre K, Rack A. 2009. LSO- based
765 single crystal film scintillator for synchrotron-
766 based hard X-ray micro-imaging. *IEEE Transac-*
767 *tions on Nuclear Science* 56(3), 1412-1418.
768
769 not cited Männik P. *The Silurian System of Esto-*
770 *nia*; 2014. pp. 123-128. Tartu.
771
772 Märss T. 1986. Silurian vertebrates of Esto-
773 nia and West Latvia. *Fossilia Baltica* 1:1–
774 104 (Russ. with Engl. sum.).
775
776 Märss T, Caldwell M, Gagnier P-Y, Goujet D,
777 Männik T, Wilson M. 1998. Distribution of Si-
778 lurian and Lower Devonian vertebrate micro-
779 remains and conodonts in the Baillie-Hamilton
780 and Cornwallis Island sections, Canadian Arc-
781 tic. *Proceedings of the Estonian Academy of*
782 *Sciences, Geology* 47(2):51-76.
783
784 not cited Märss T, Männik P. 2013. Revi-
785 sion of Silurian vertebrate biozones and
786 their correlation with the conodont succes-
787 sion. *Estonian Journal of Earth Sciences*
788 62(4):181-204.
789
Ørvig T. 1951. Histologic studies of Placo-
derms and fossil Elasmobranchs. I: The en-
doskeleton, with remarks on the hard tissues

of lower vertebrates in general. *Arkiv för Zoologi* 2(2):321–454.

not cited Ørvig T. 1957. Paleohistological notes. 1. On the structure of the bone tissue in the scales of certain Palaeonisciformes. *Arkiv för Zoologi* 10(12):481–490.

Ørvig T. 1977. A survey of odontodes ('dermal teeth') from developmental, structural, functional, and phyletic points of view. In: Andrews SM, Miles RS, Walker AD (Eds.), Problems in Vertebrate Evolution. *Linnean Society Symposium Series* 4:53–57. town, publisher

Otto M. 1991. Zur systematischen Stellung der Lophosteiden (Obersilur, Pisces inc. sedis). *Paläontologische Zeitschrift* 65:345-350.

Pander CH. 1856. *Monographie der fossilen Fische des silurischen Systems der Russisch- Baltischen Gouvernements*. St. Petersburg. publisher, pp.?

not cited Qu Q, Zhu M, Wang W. 2013a. Scales and dermal skeletal histology of an early bony fish *Psarolepis romeri* and their bearing on the evolution of rhombic scales and hard tissue. *PLoS One* 8(4) DOI: 10.1371/journal.pone.0061485.

Qu Q, Sanchez S, Blom H, Tafforeau P, Ahlberg PE. 2013b. Scales and tooth whorls of ancient fishes challenge distinction between external and oral 'teeth'. *PloS One* 8: e71890 DOI:10.1371/journal.pone.0071890.

796
797
798   not cited Qu Q, Blom H, Sanchez S, Ahl-
799   berg PE. 2015a. Three-Dimensional Virtual
800   Histology of Silurian Osteostracan Scales
801   Revealed by Synchrotron Radiation Mi-
802   crotomography. *Journal of Morphology*
803   276:873–888 DOI:10.1002/jmor.20386.
804
805   Qu Q, Haitina T, Zhu M, Ahlberg, PE.
806   2015b. Genomic and fossil data illuminate
807   the origin of enamel. *Nature* 526:108-111
808   DOI:10.1038/nature15259.
809
810   Qu Q, Sanchez S, Zhu M, Blom H, Ahlberg
811   PE. In press. The origin of novel features by
812   changes in developmental mechanisms: on-
813   togeny and three-dimensional microanatomy
814   of polyodontode scales of two early osteich-
815   thyans. *Biological Reviews*.
816
817   Rohon JV. 1893. Die Obersiluischen Fische
818   von Oesel. Theil 2. *Mémoires de
819   l'Académie Impériale des Sciences de St.
820   Pétersbourg* 41, pp.1-124.
821
822   Sanchez S, Ahlberg PE, Trinajstic KM,
823   Morone A, Tafforeau P. 2012. Three-
824   Dimensional Synchrotron Virtual Paleo-
825   histology: A New Insight into the World
826   of Fossil Bone Microstructures. *Micros-
827   copy and Microanalysis* 18:1095–1105,
828   DOI:10.1017/S1431927612001079.
829
830   not cited Sanchez S, Dupret V, Tafforeau P,
831   Trinajstic K, Ryll B, Gouttenoire P-J, Wret-
832   man L, Zylberberg L, Peyrin F, Ahlberg PE.
833   2013. 3D microstructural architecture of mus-
834   cle attachments in extant and fossil verte-
835   brates revealed by synchrotron microtomog-
836   raphy. *Plos One* 8: e56992.
837
844   not cited Sanchez S, Tafforeau P, Ahlberg PE.
        2014. The humerus of *Eusthenopteron*: a puz-
        zling organization presaging the establishment
        of tetrapod limb bone marrow. *Proceedings of
        the Royal Society of London* B 281: 20140299.

Schultze, H.-P. 2015. Scales, Enamel, Cosmine, Ganoine, and Early Osteichthyans. *Comptes Rendus Palevol* 83-102 DOI:10.1016/j.crpv.2015.04.001.

Schultze H-P, Märss T. 2004 Revisiting *Lophosteus* Pander 1856, a primitive osteichthyan. *Acta Universitatis Latviensis* 674:57–78.

not cited Tafforeau P, Boistel R, Boller E, Bravin A, Brunet M, Chaimanee Y, Cloetens P, Feist M, Hoszowska J, Jaeger J-J, Kay RF, Lazzari V, Marivaux L, Neil A, Nemoz C, Thibault X, Vignaud P, Zabler S. 2006. Applications of X-ray synchrotron microtomography for non- destructive 3D studies of paleontological specimens. *Applied Physics A Materials Science and Processing* 83:195–202.

Trinajstic K. 1999. Scale morphology of the Late Devonian palaeoniscoid Moythomasia durgaringa Gardiner and Bartram, 1997. *Alcheringa* 23:9-19.

Valiukevičius J, Burrow CJ. 2005. Diversity of tissues in acanthodians with *Nostolepis*- type histological structure. *Acta Palaeontologica Polonica* 50:635–649.

Warren A, Currie BP, Burrow C, Turner S. 2000. A redescription and reinterpretation of *Gyracanthides murrayi* Woodward 1906 (Acanthodii, Gyracanthidae) from the Lower

845
846
847 Carboniferous of the Mansfield Basin, Vic-
848 toria, Australia. *Journal of Vertebrate*
849 *Paleontology* 20(2):225-242.
850
851 not cited Yu X-B. 1998. A new
852 porolepiform-like fish, *Psarolepis*
853 *romeri*, gen. et sp. nov. (Sarcopte-
854 rygii, Osteichthyes) from the Lower
855 Devonian of Yunnan, China. *Jour-*
856 *nal of Vertebrate Paleontology*
857 18(2):261-274.
858
859 Zhu M, Yu X, Janvier P. 1999. A primitive fossil
860 fish sheds light on the origin of bony fishes.
861 *Nature* 397:607–610 DOI:10.1038/nature17594.
862
863 Zhu M, Yu X, Ahlberg PE, Choo B, Lu J,
864 Qiao T, Qu Q, Zhao W, Jia L, Blom H, Zhu
865 Ya. 2013. A Silurian placoderm with oste-
ichthyan-like marginal jaw bones. *Nature*
502(7470):188-193.

Zhu M, Zhao W, Jia L, Lu J, Qiao T, Qu Q.
2009. The oldest articulated osteichthyan reveals
mosaic gnathostome characters. *Nature*
458:469–474 DOI:10.1038/nature07855.

Žigaitė Ž, Fadel A, Blom H, Pérez-Huerta
A, Jeffries T, Märss T, Alhberg PE. 2015.
Rare earth elements (REEs) in vertebrate
microremains from the Upper Pridoli Ohe-
saare beds of Saaremaa Island, Estonia: ge-
ochemical clues to palaeoenvironment. *Es-*
tonian Journal of Earth Sciences 64(1):115-
12

866
867
868
869
870
871
872
873
874
875
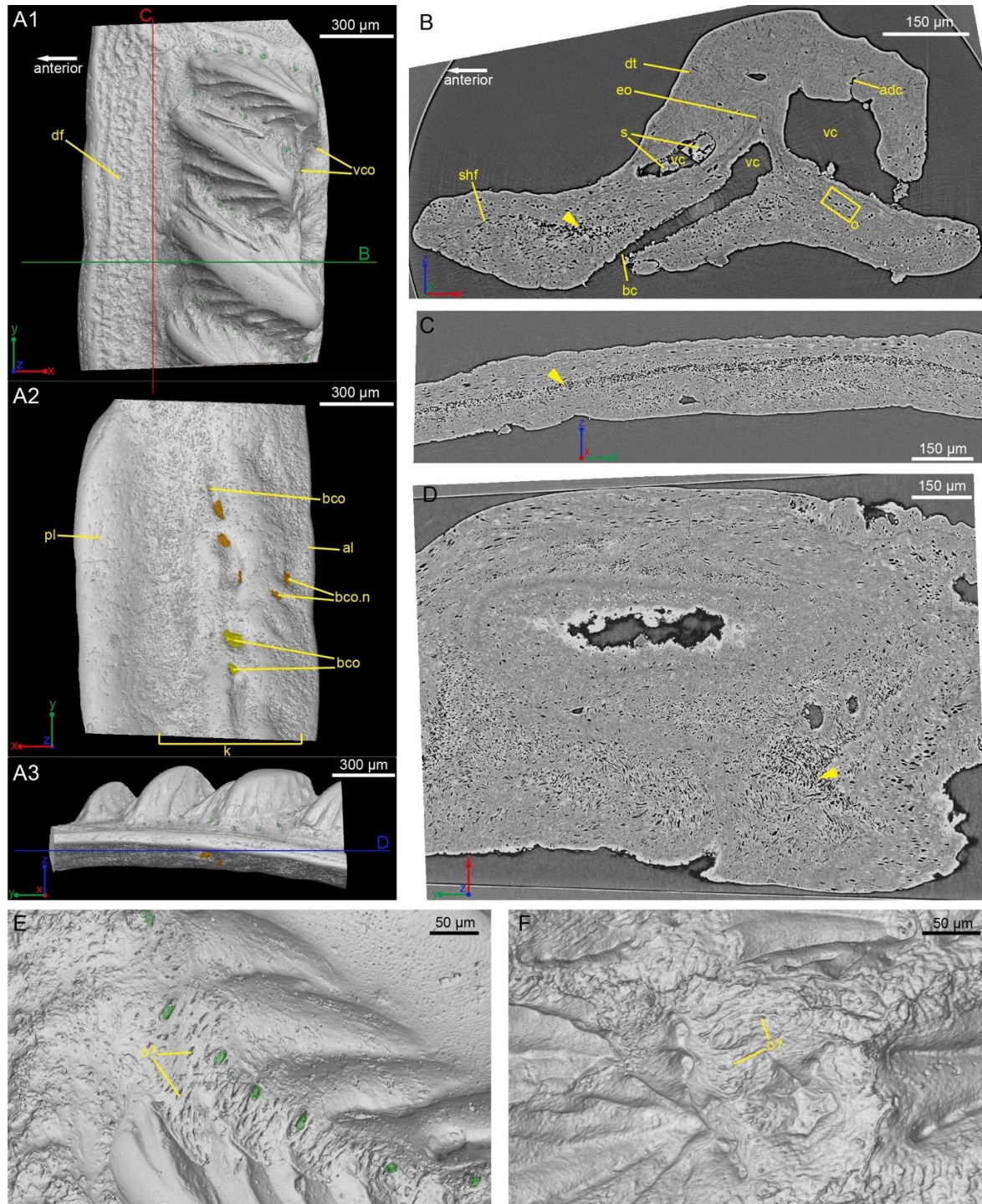
Figure 1 The scanned scale (GIT 727-1) of *Lophosteus superbus*.

(A) Scale in crown (A1), basal (A2) and anterior (A3) view. Red and green lines in A3 mark the cutting planes for the virtual thin sections in B, C; Blue line in A3 marks the cutting plane for the virtual thin section in D. **(B)** Vertical anteroposterior virtual thin section showing the embedded odontode (eo) and other histological structures. Arrow head marks the same loose region in B, C and D. **(C)** Vertical dorsoventral virtual thin section showing the continuous loose region in the middle of the bony base. **(D)** Horizontal virtual thin section. **(E)** Zoom-in of a region between two crown ridges of (GIT 727-1) showing bone-like tissue and osteocyte- like spaces. **(F)** Zoom-in of a region surrounded by crown ridges of a *Romundina stellina* scale (NRM-PZ P.15952), rendered in VG Studio MAX 2.2 using data from not in references Rücklin and Donoghue, 2015.

878
879
880
881
882
883
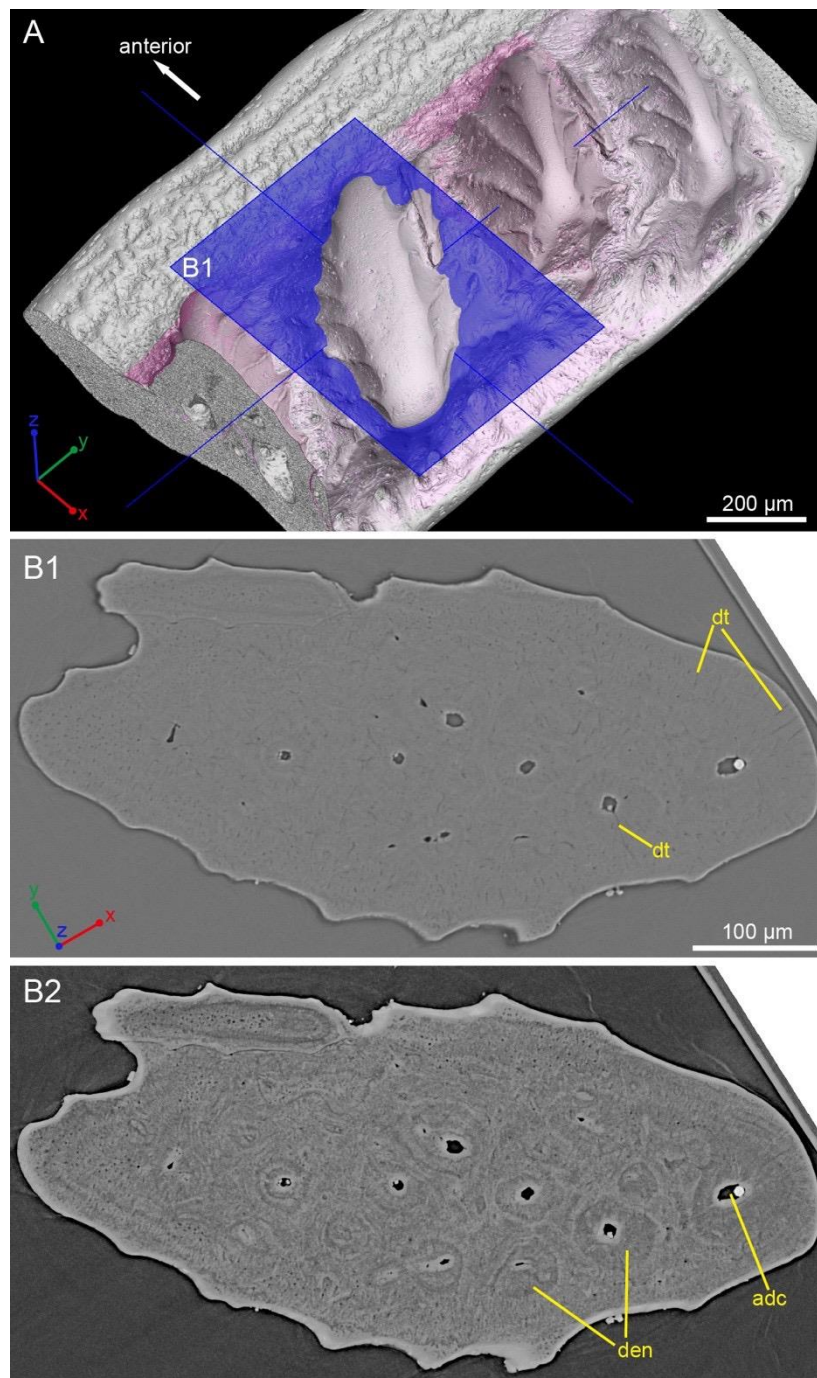
Figure 2 Histological detail of a large odontode of (GIT 727-1).

(A) Posteroventral view of the scale crown, showing the cutting plane of the virtual thin section in B1 and B2, C. **(B1)** Horizontal virtual thin section cutting through a large dental ridge of the crown, with default contrast setup in VGStudio MAX 2.2. **(B2)** The same

section as in B but the image contrast is increased in VGStudio MAX 2.2 to show denteons in a large odontode.
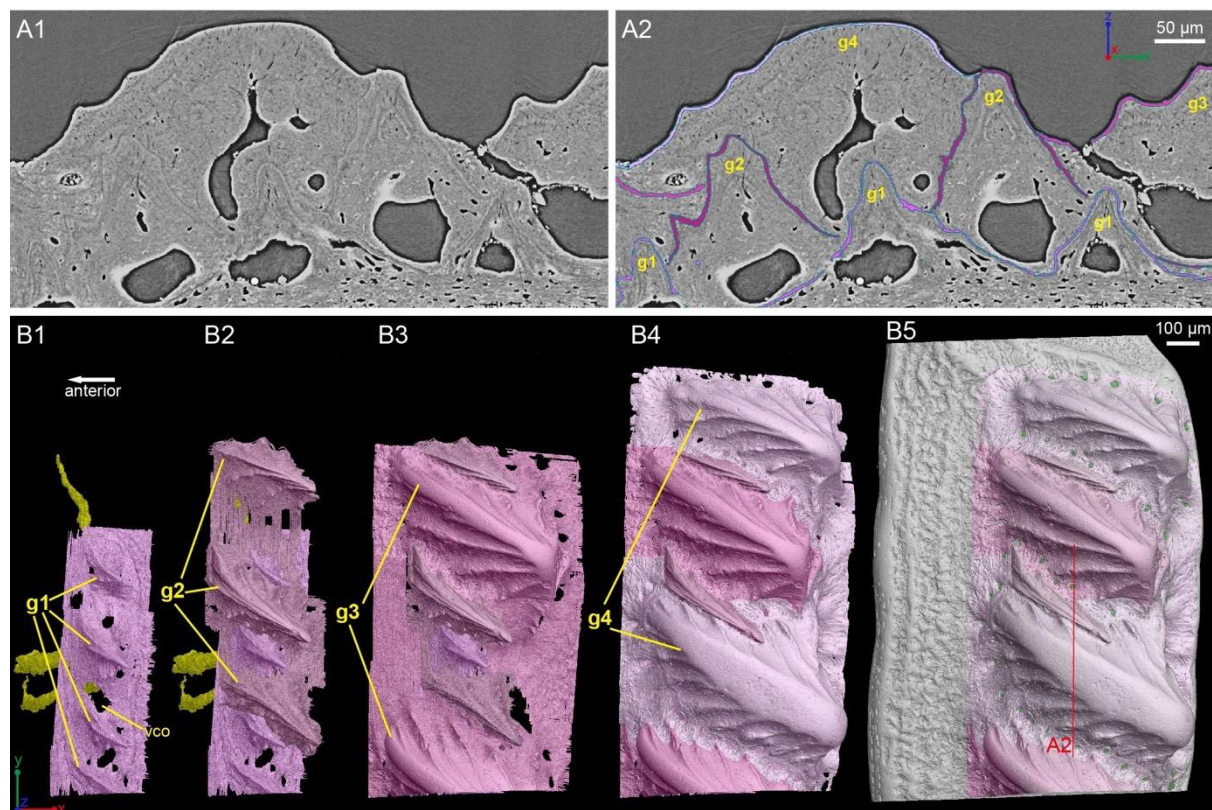
Figure 3 Segmentation of the virtual thin sections of the *Lophosteus* scale and the growth history of the scale crown. **(A)** Vertical dorsoventral virtual thin section showing embedded odontodes in the crown (A1) and their surfaces selected in VG VGStudio MAX 2.2. **(B)** Rendered odontodes in sequential order showing the growth history of the scale, crown view. Red line in B5 marks the cutting plan of the virtual thin section in A.

PeerJ

890
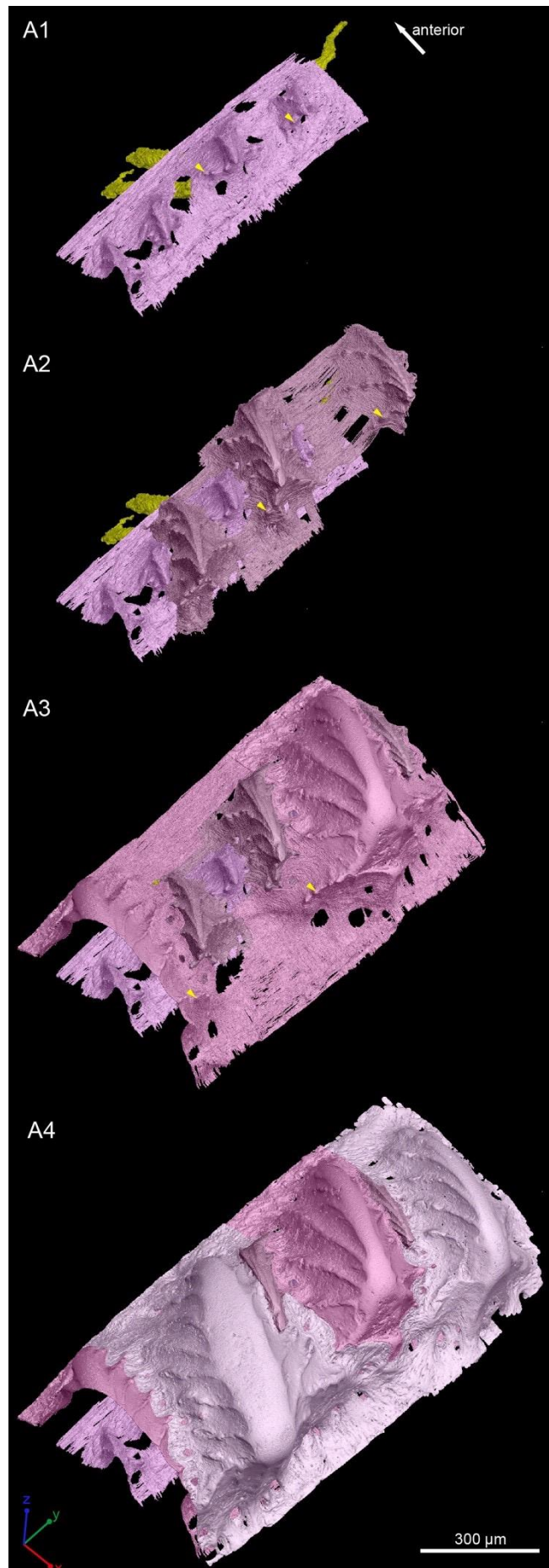
Figure 4 Growth history of the scale crown in posteroventral view. Arrow heads mark the small nodules on the ridgelets of embedded odontodes.
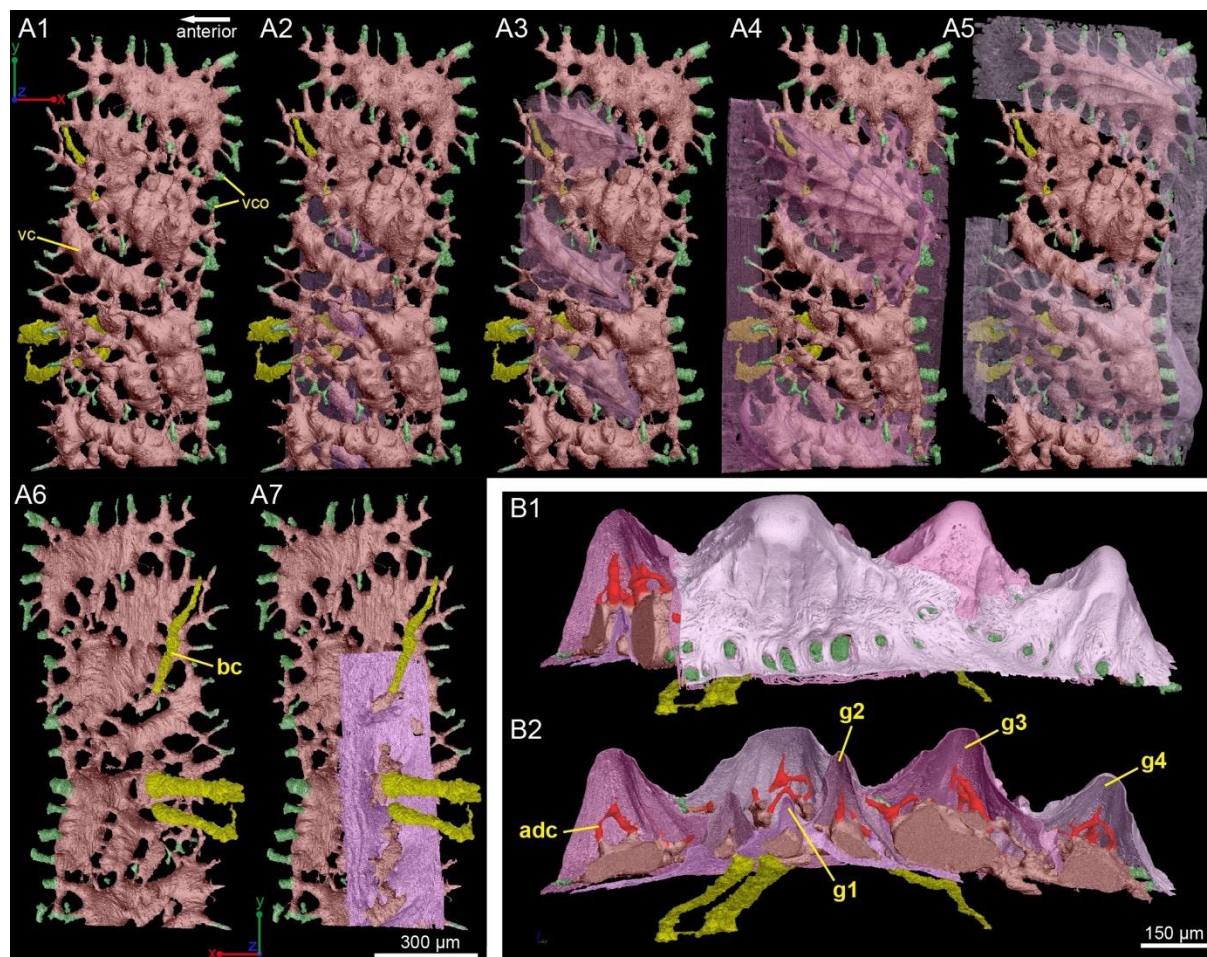
Figure 5 Three-dimensional vasculature of the *Lophosteus* scale. **(A)** Crown view (A1-A5) and basal view (A6-A7). Four generations of odontodes are rendered transparent to show their underlying vascular canals in A2-A5. The first generation of odontodes is shown in A7, with all basal canals below these odontodes. **(B)** Posterolateral view with rendered surfaces of odontodes.

891
892
893
894
895
896
897
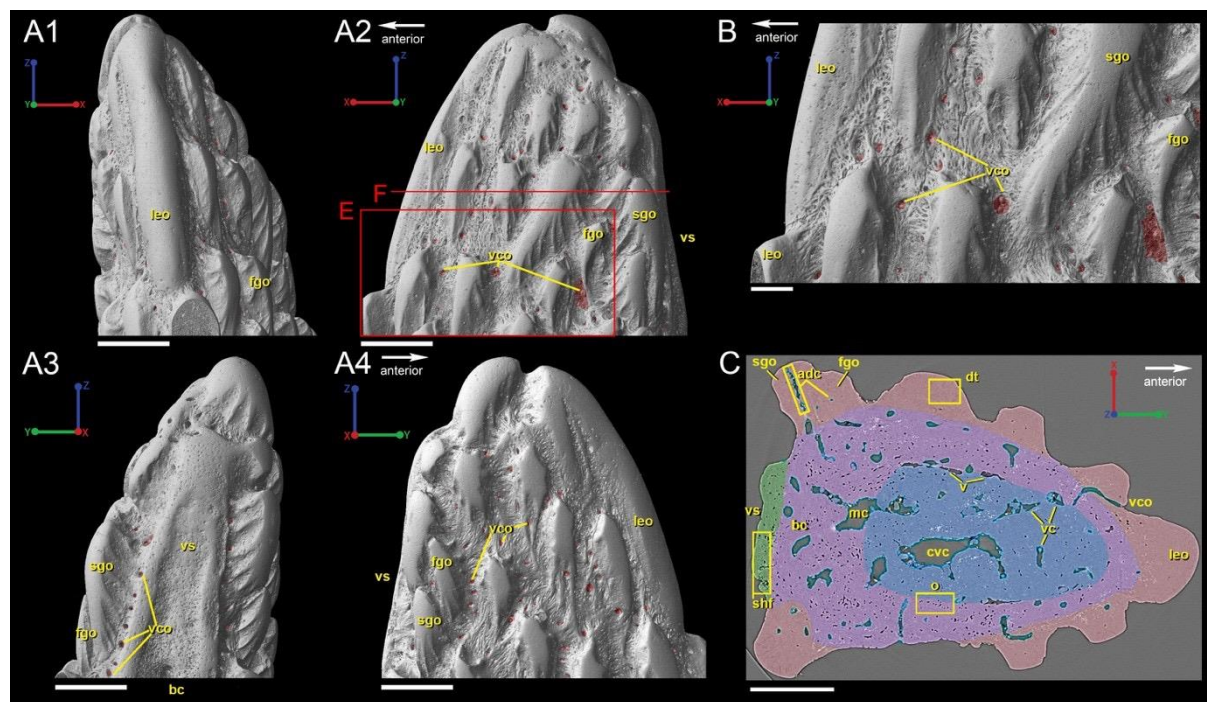
Figure 6 3D renderings of the tip of the fin spine of *Lophosteus superbus* (**GIT 727-2**) in **(A1)** dorsal, **(A2)** left lateral, **(A3)** ventral, and **(A4)** right lateral views. Scale bar for **(A1-A4)** is 300μm. **(B)** Magnified view of a portion of the left lateral view of the spine, indicated in **(A2)** by the red box. Scale bar is 100μm. **(C)** Virtual thin section in transverse view of the fin spine indicated by the red line in **(A2)**, which highlights its general histological features. The color coding denotes zones (boundaries are approximations) of the spine tip, including bone with fewer bone cells spaces (blue), bone with many cell spaces (purple), dentine (red), and Sharpey's fibers (green). Scale bar is 200μm.

911
912
913
914
915
916
917
918
919
920
921
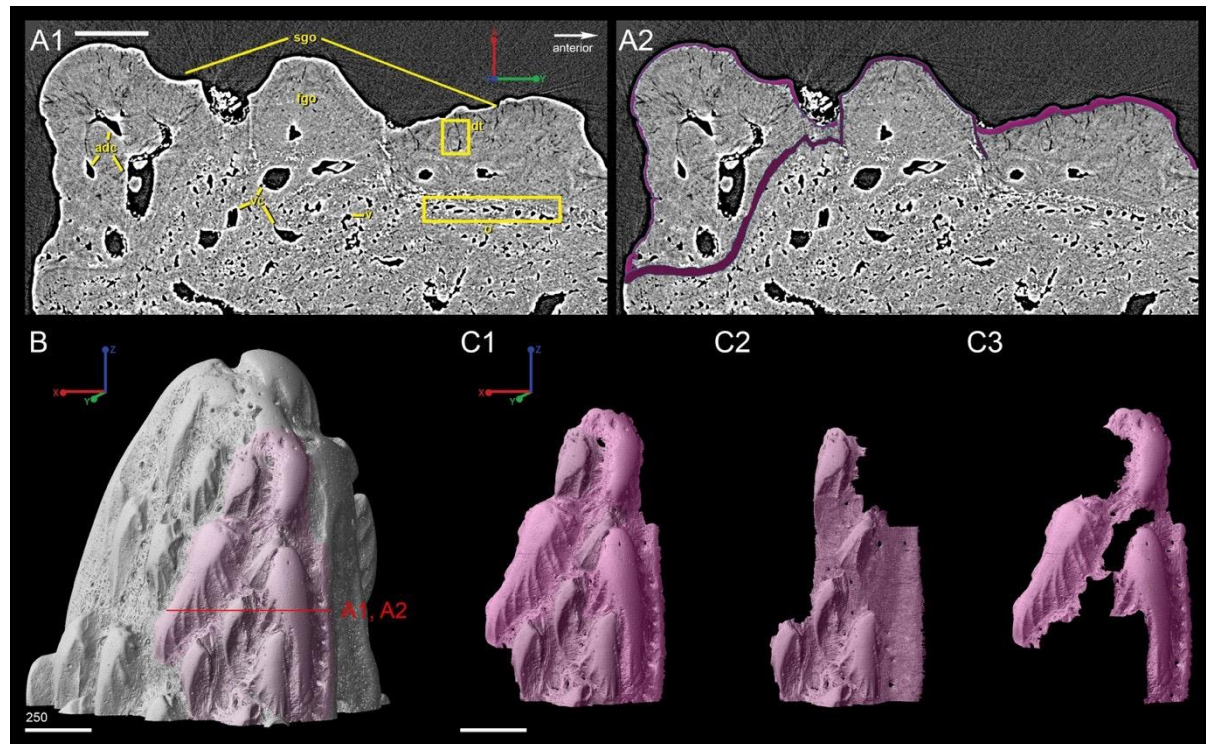
Figure 7 Virtual thin sections of lateroventral surface of the spine of *L. superbus* (**GIT 727-2**) showing **(A1)** the morphology of the area and **(A2)** highlighting first and second generation odontodes. A1 and A2 are the same image and share the same coordinate system and scale bar. Scale bar is 80μm. **(B)** Rendered surface of the entire tip of the fin spine showing the location in red of the A1 and A2 virtual thin sections. The pink portion of the surface shows the location of the partially buried odontodes. **(C1)** separates the pink region from the rest of the 3D rendering while **(C2)** isolates the first-generation odontodes and buried surface (dark pink) and **(C3)** shows the position and morphology of second-generation odontodes (light pink). B and C1-3 share coordinate system and scale bars. Scale bars are 200μm.
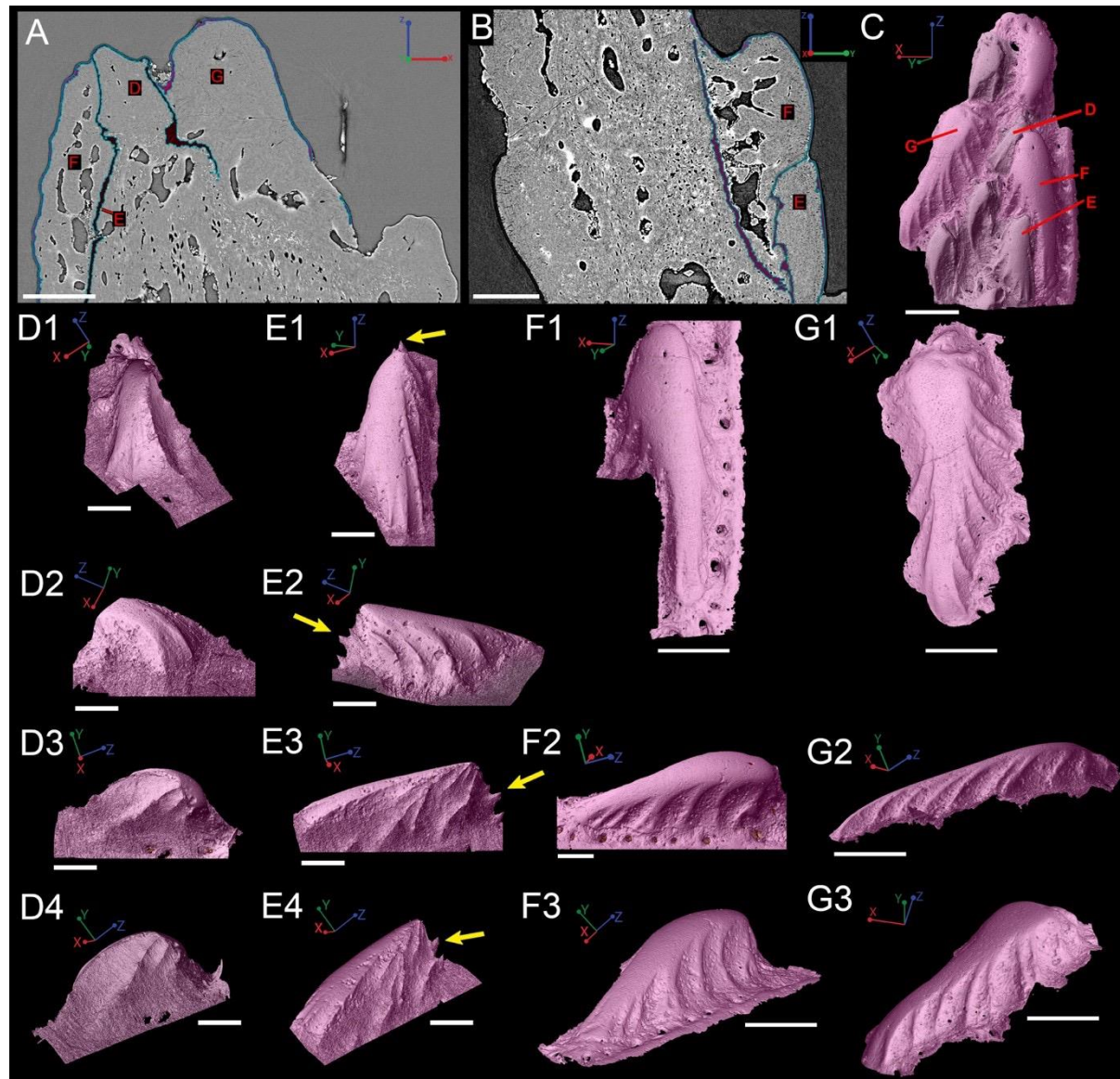
Figure 8 Virtual thin sections of the *Lophosteus* (**GIT 727-2)** spine taken in **(A)** frontal and (B) sagittal planes and a **(C)** 3D rendering of the entire area with odontodes (D-G) marked to show position to each other. Scale bars are as follows: (A) is 150µm, (B) is 200µm, and (C) is 250µm. 3D renderings of individual first-generation odontodes to show the morphology and ornamentation in **(D1)** dorsal, **(D2, D3)** lateral, and **(D4)** oblique lateral views. **(E1-4)** illustrates the same, but with a different first-generation odontode. Yellow arrow indicates the buried denticles

on first generation odontodes. Scale bars for D and E are 75µ. **(F1)** shows the morphology of a second-generation odontode in dorsal view, in addition to **(F2)** lateral and **(F3)** oblique lateral views. Scale bars for F1& F3 are 150µm and F2 is 100µm. **(G1-3)** illustrates the morphology of another second-generation odontode in the same orientation, as the odontode figured in F. Scale bars are 150µm.
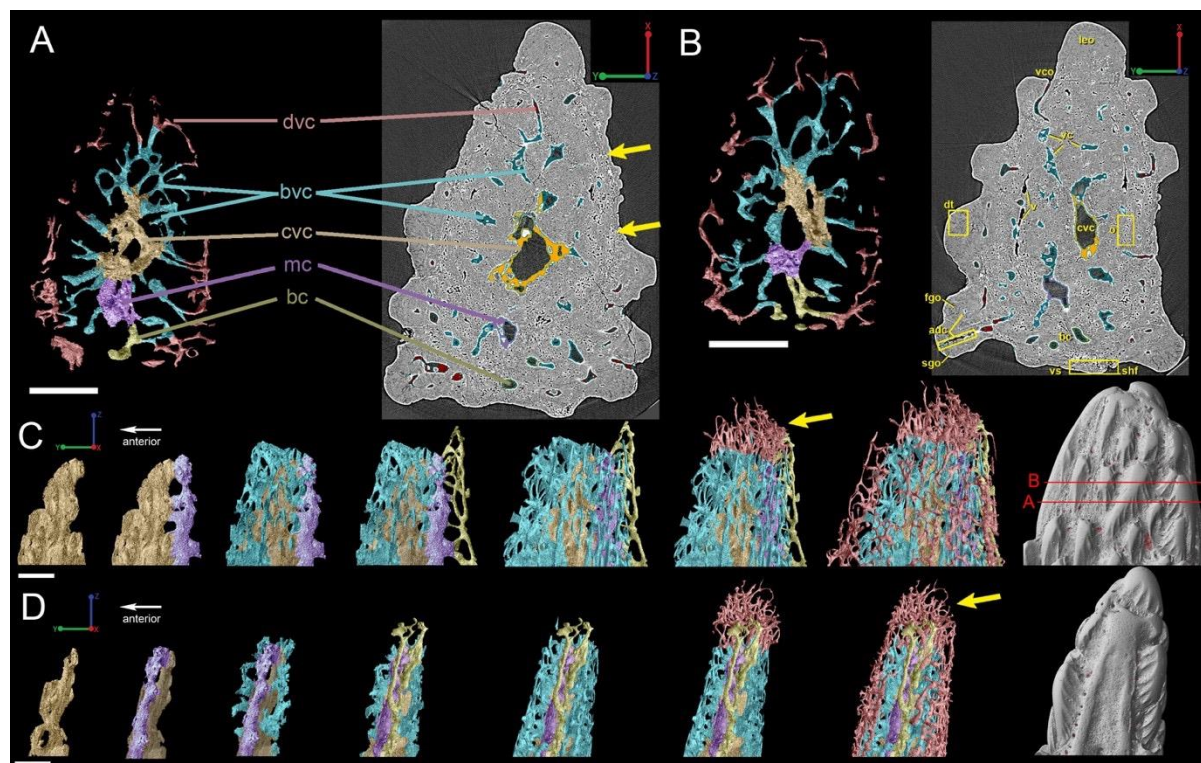
Figure 9 Breakdown of the vascularization within the tip of the fin spine of *Lophosteus* (**GIT 727-2).** (**A**) and (**B**) are cross-sections of 3D renderings and scan data of slices 472-680 and 786-984 (thin sections are slices 580 and 880), respectively, to show how each layer of canals relates to each other. Orange: central vascular canal, cvc; Light blue: 1st tier canals, 1st; Dark Blue: median canal, mc; Yellow: basal canal, bc; Purple: 2nd tier canals, 2nd; Pink: 3rd tier canals, 3rd. 3D renderings of the surface of the spine also included in white at the end of each vascular canal. Color scheme is the same throughout figure. Scale bars for (A) and (B) are 250μm. (**C**) left lateral and (**D**) posterior views. The locations of the virtual thin sections and renderings are labeled in red on the surface rendering of the spine in (C). Scale bars for (C) and (D) are 300μm. Yellow arrows explained in text.
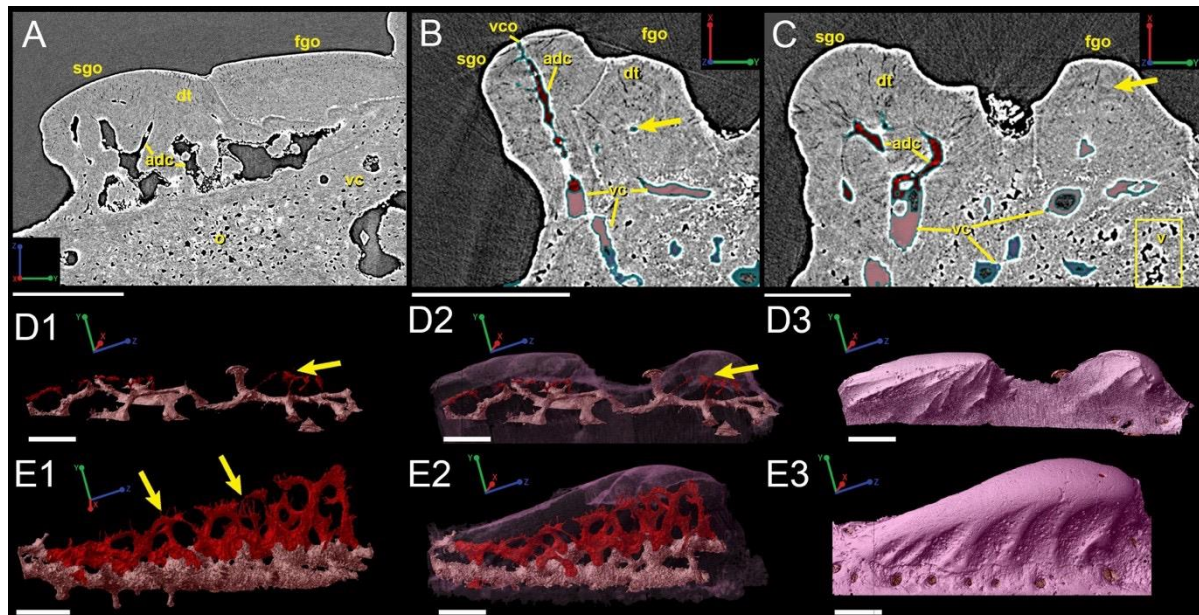
Figure 10 Virtual thin sections and 3D renderings of odontode morphology and vascularization. **(A)** shows the sagittal view of the network of ascending canals within a single odontode and **(B)** and **(C)** illustrate the location of the ascending canals (red) in relation to the outer layer of vascular canals (pink). Scales bars are 200µm. **(D1)** is a 3D rendering of the ascending canals (red) and the outer tier of canals of the spine (pink) in a second- generation odontode. **(D2)** shows the semi-transparent surface of the same odontode and **(D3)** shows the full surface of the odontode. Scale bars are 100µm. **(E1-3)** shows the same as D1-3, but in two-first-generation odontodes. Scale bars are 100µm. Yellow arrows explained in text.
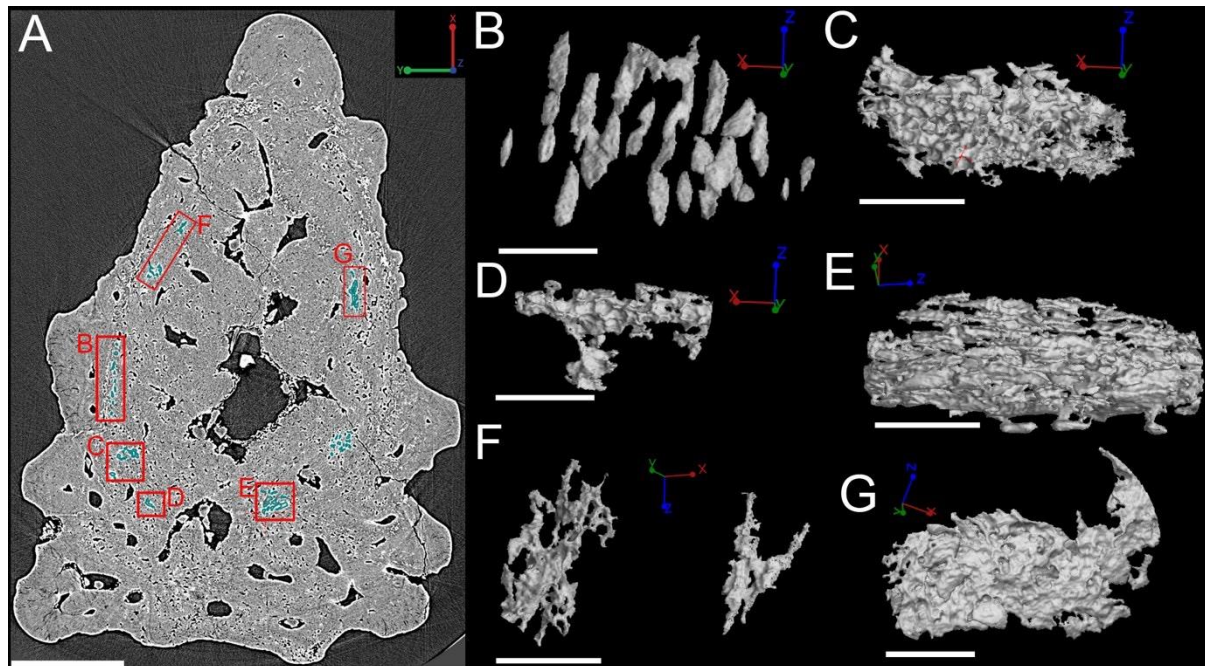
966
967
968
969
970
971
972
973

Figure 11 (**A**) Synchrotron scan slice through the *Lophosteus* fin spine showing the location and organization of different cell and void spaces. Scale bar is 200μm. Modeled cell spaces include (**B**) osteocytes and (**C-F**) unidentifiable void spaces. Scale bars are 45μm.
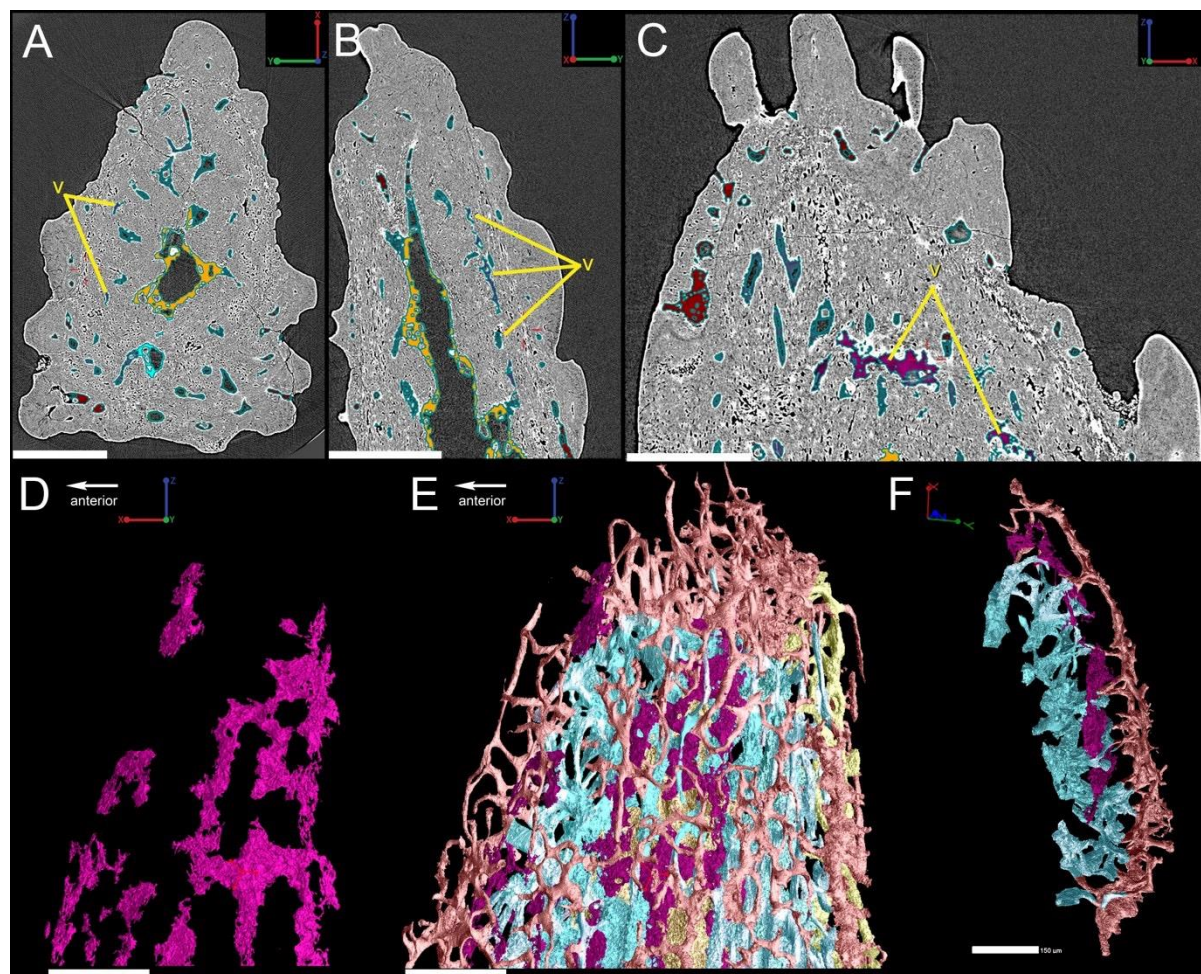
Figure 12 (**A-C**) Synchrotron scan slices of
the Lophosteus spine to show the location,
morphology, and organization of a layer of
void spaces (pseudo-canals?). (**D**) 3D render-
ing of the void spaces/psuedocanals and how
they fit together with the rest of the vasculari-
zation in
(**E**) lateral view of the entire specimen and
in (**F**) cross-section. Scale bars for (A-E)
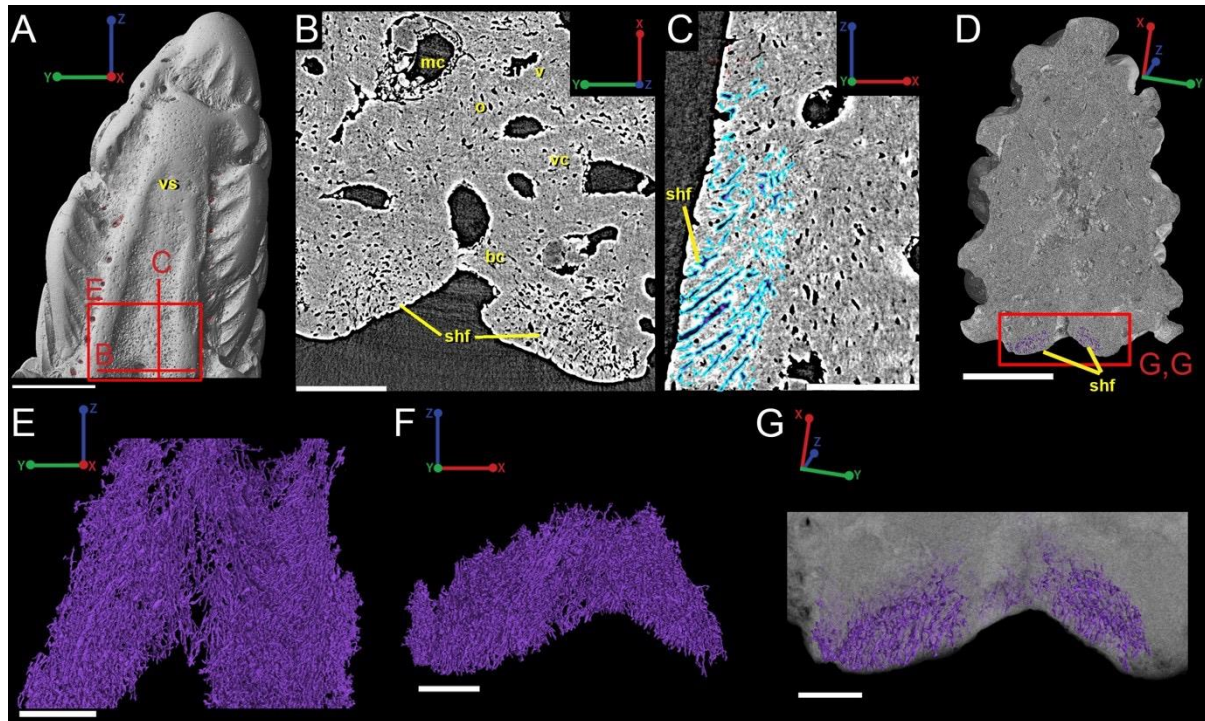are 250μm and scale are for (F) is 150μm.

Figure 13 (A) 3D rendering of the ventral surface of the Lophosteus spine. Red lines indicating the location of the slices for (B) and (C). Scale bar 300μm. The location of Sharpey's fibers in the ventral portion of the spine in **(B)** transverse and **(C)** sagittal sections. Fibers are highlights in purple in (C). Scale bar for (B) is 200μm and (C) is 100μm. **(D)** Transverse posterior view of the fin spine to illustrate the position of the Sharpey's fibers. Scale bar is 350μm. 3D renderings of the Sharpey's fibers in **(E)** ventral view and **(F)** transverse posterior view. Scale bar for (E) is 80μm and (F) is 70μm. (G) Cross-section of (F) with semi-transparent surface. Location of (E-G) indicated by the red boxes in (A) and (D). Scale bar is 70μm.